RSC Advances

PAPER

View Article Online
View Journal | View Issue

Cite this: *RSC Adv.*, 2024, **14**, 7964

Anticancer evaluations of iodoquinazoline substituted with allyl and/or benzyl as dual inhibitors of EGFR^{WT} and EGFR^{T790M}: design, synthesis, ADMET and molecular docking†

Ahmed K. B. Aljohani, [a] Khaled El-Adl, *[bc] Basmah Almohaywi, [d] Omar M. Alatawi,[e] Marwa Alsulaimany,[f] Ahmed El-morsy,[g] Sara A. Almadani,[h] Hussam Y. Alharbi, [i] Majed S. Aljohani,[i] Felemban Athary Abdulhaleem M,[j] Hanan E. M. Osman[jk] and Samy Mohamady[l]

Fifteen new iodoquinazoline derivatives, **5a,b** to **18**, are reported in this study and their anticancer evaluation as dual inhibitors of EGFR^{WT} and EGFR^{T790M}. The new derivatives were designed according to the target of structural requirements of receptors. Cytotoxicity of our compounds was evaluated against MCF-7, A549, HCT116 and HepG2 cell lines using MTT assay. Compounds **18**, **17** and **14b** showed the highest anticancer effects with IC_{50} = 5.25, 6.46, 5.68 and 5.24 μM, 5.55, 6.85, 5.40 and 5.11 μM and 5.86, 7.03, 6.15 and 5.77 μM against HepG2, MCF-7, HCT116 and A549 cell lines, respectively. The eight highly effective compounds **10**, **13**, **14a**, **14b**, **15**, **16**, **17** and **18** were inspected against VERO normal cell lines to evaluate their cytotoxicity. Our conclusion was that compounds **10**, **13**, **14a**, **14b**, **15**, **16**, **17** and **18** possessed low toxicity against VERO normal cells with IC_{50} increasing from 43.44 to 52.11 μM. All compounds were additionally assessed for their EGFR^{WT} and EGFR^{T790M} inhibitory activities. Additionally, their ability to bind with EGFR^{WT} and EGFR receptors was confirmed by molecular docking. Compound **17** exhibited the same inhibitory activity as erlotinib. Compounds **10**, **13**, **14b**, **16** and **18** excellently inhibited VEGFR-2 activity with IC_{50} ranging from 0.17 to 0.50 μM. Moreover, compounds **18**, **17**, **14b** and **16** remarkably inhibited EGFR^{T790M} activity with IC_{50} = 0.25, 0.30, 0.36 and 0.40 μM respectively. As planned, compounds **18**, **17** and **14b** showed excellent dual EGFR^{WT}/EGFR^{T790M} inhibitory activities. Finally, our compounds **18**, **17** and **14b** displayed good *in silico* ADMET calculated profiles.

Received 19th January 2024
Accepted 16th February 2024

DOI: 10.1039/d4ra00502c

rsc.li/rsc-advances

1. Introduction

The globally most fatal type of all cancers is lung cancer. Every year 7 million people die due to cancer. Lung cancer is estimated to account for 25% of these deaths.[1] Lung cancer is categorized into small cell lung cancer (SCLC) and non-small cell lung cancer (NSCLC).[2] NSCLC is the fatal type of lung cancer with approximately 1.5 million recorded cases with below 20% survival rate. Targeted therapy intended at signaling pathways and cancer-particular molecules showed fewer side effects than chemotherapy.[3] In anticancer therapy, one of the most important targets is PTKs (protein tyrosine kinases), as they modify the signaling pathway of growth factors.[4]

[a]*Pharmacognosy and Pharmaceutical Chemistry Department, College of Pharmacy, Taibah University, Al-Madinah Al-Munawarah 41477, Saudi Arabia. E-mail: eladlkhaled74@azhar.edu.eg; khaled.eladl@hu.edu.eg; eladlkhaled74@yahoo.com*

[b]*Chemistry Department, Faculty of Pharmacy, Heliopolis University for Sustainable Development, Cairo, Egypt*

[c]*Pharmaceutical Medicinal Chemistry and Drug Design Department, Faculty of Pharmacy (Boys), Al-Azhar University, Nasr City, 11884, Cairo, Egypt*

[d]*Department of Pharmaceutical Chemistry, College of Pharmacy, King Khalid University, Abha 61421, Saudi Arabia*

[e]*Department of Chemistry, Faculty of Science, University of Tabuk, Tabuk 47512, Saudi Arabia*

[f]*Department of Pharmacognosy & Pharmaceutical Chemistry, College of Pharmacy, Taibah University, Medina 42353, Saudi Arabia*

[g]*Pharmaceutical Chemistry Department, College of Pharmacy, The Islamic University, Najaf, Iraq*

[h]*Department of Pharmacology and Toxicology, College of Pharmacy, Taibah University, Medina 42353, Saudi Arabia*

[i]*Department of Chemistry, Faculty of Science, Taibah University, Yanbu, Saudi Arabia*

[j]*Biology Department, Faculty of Science, Umm Al-Qura University, Makkah 21955, Saudi Arabia*

[k]*Botany and Microbiology Department, Al-Azhar University, Cairo 11651, Egypt*

[l]*Pharmaceutical Chemistry Department, Faculty of Pharmacy, The British University in Egypt, Cairo, Egypt*

† Electronic supplementary information (ESI) available. See DOI: https://doi.org/10.1039/d4ra00502c

PTKs play an important role in controlling the cancer physiological cycle and are found on cell membranes of living organisms.[5] EGFR is one of the PTKs that was documented to be the most vital target for the managing of growth, proliferation, and differentiation of cancers.[6] Most of the NSCLC therapeutic agents/EGFR inhibitors have a shared structure of quinazoline (Fig. 1).[1] In the first year of treatment with these drugs, more than 50% of the patients developed resistance by T790M mutation.[7] As such, many second-generation EGFR inhibitors, such as afatinib and dacomitinib (Fig. 1), were designed and developed to manage the resistance caused by the T790M mutation.[1] The reported objective was not attained due to serious side effects produced by second-generation EGFR inhibitors, such as diarrhea and skin rashes. Many third-generation NSCLC therapeutic agents/EGFR inhibitors, such as AZD9291 and WZ4002 (Fig. 1), were designed and synthesized to manage the developed resistance caused by $EGFR^{T790M/L858R}$ mutations.[8] This study targets the computational design of new $EGFR^{WT}/EGFR^{T790M}$ inhibitors with enhanced inhibitory effects, as well as a docking study and prediction of pharmacokinetic properties of these new EGFR inhibitors.

The current research is an extension to our earlier studies[15–30] to achieve anticancer agents. This study showed the effectiveness of hybridization between iodoquinazolinone and different moieties to produce anticancer agents targeting $EGFR^{WT}$ and $EGFR^{T790M}$. We obtained a new series of iodoquinazolinone joined to different moieties through acetamide linker as dual $EGFR^{WT}/EGFR^{T790M}$ inhibitors for cancer treatment against A549, HCT116, MCF-7 and HepG2. *In silico* molecular docking study was performed for our derivatives to discover their binding modes in EGFR active sites and/or predict their ADMET properties.

1.1. Rationale and structure-based design

In this research, we used iodo-substitution of quinazoline derivatives as anticancer agents due to iodine high atomic number, ease of attachment to organic compounds, and the specificity of its uptake by the human body, and radioactive isotopes of iodine can also be used to treat thyroid cancer. Moreover, there are many approved drugs containing iodo substitutions, such as 2-iodo-4′-methoxychalcone, amiodarone and iodochlorhydroxyquinoline (clioquinol).[31] Our compounds were constructed according to the structural requirements of inhibitors of EGFR. A new series of iodoquinazolines was synthesized through bioisosteric variations of erlotinib at four points: (1) a flat hetero-aromatic system that occupies the adenine binding pocket, (2) a terminal hydrophobic head (occupying hydrophobic region I) which was replaced by allyl and/or benzyl moieties, (3) an NH group (as HBD and/or HBA) which was replaced in our derivatives with a carbonyl group as the HB acceptor, and (4) a hydrophobic tail (occupying hydrophobic region II) which was replaced with different side chain moieties (Fig. 2 and 3).[32–37]

2. Results and discussion

2.1. Chemistry

The synthetic pathways for derivatives **5a,b** to **18** are illustrated in Schemes 1 and 2. This started with the reaction of chloroacetyl chloride with suitable amine **Ia–d** to give corresponding chloroacetamide **IIa–d**.[38,39] The chloroactamide **IIa** underwent reaction with appropriate methyl and/or ethylamine according to the mixed anhydride procedure[39] to give derivatives **IIIa,b**

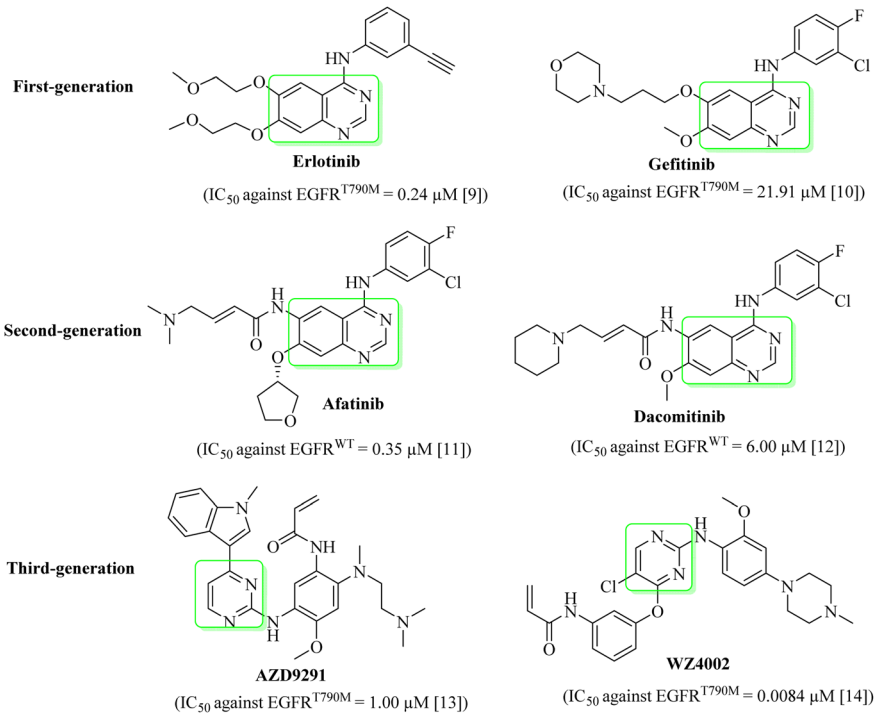

Fig. 1 Quinazoline- and pyrimidine-based EGFR inhibitors.[9–14]

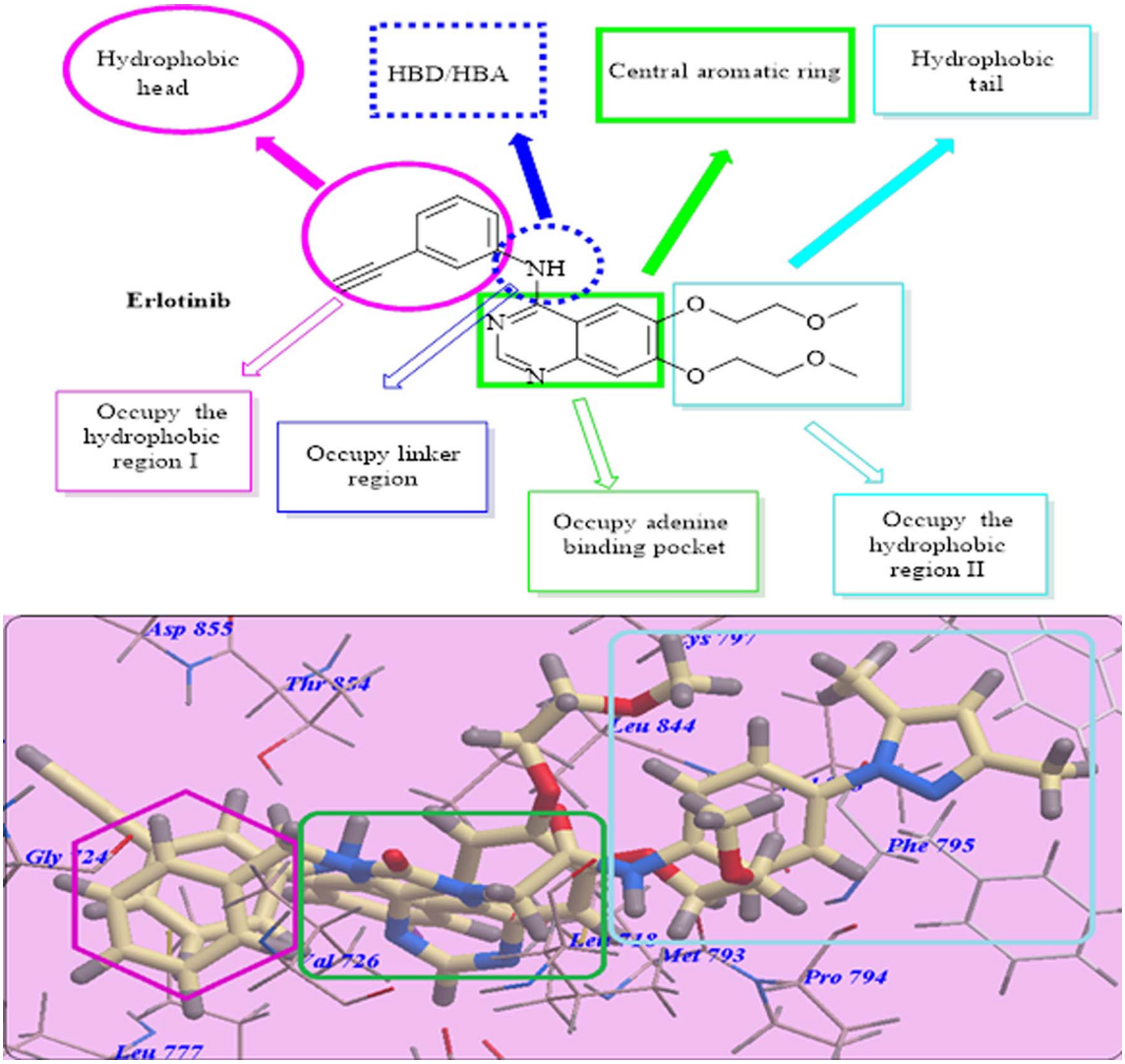

Fig. 2 Structural requirements for erlotinib as a reported EGFR-TK inhibitor.

correspondingly. Reaction of anthranilic acid (**1**) with iodine afforded 5-iodoanthranilic acid (**2**) which underwent reaction with allyl bromide to give the corresponding *N*-allyl derivative (**3**).[40] Fusion of 5-iodo-*N*-allylanthranilic acid (**3**) with urea afforded 6-iodo-1-allylquinazoline-2,4(1*H*,3*H*)-dione (**4**).[40] *In situ* reaction of 6-iodo-1-allylquinazoline-2,4(1*H*,3*H*)-dione (**4**) with the appropriate chloroacetamide **IIIa,b** afforded corresponding benzamide derivatives **5a,b**. ^{1}H-NMR spectrum of derivative **5b** as an example revealed characteristic bands for the new *N*-allyl group at 5.10–5.18 for C**H**$_2$CH and C**H**$_2$=CH and at 5.88–5.92 for C**H**=CH$_2$. Moreover, it showed signals for C**H**$_3$ and C**H**$_2$ at 1.21–125 and 3.82–3.88, respectively. ^{13}C-NMR is also consistent with the formed structure. Moreover, reaction of 6-iodo-1-allylquinazoline-2,4(1*H*,3*H*)-dione (**4**) with the appropriate chloroacetamide **IIb,c** afforded corresponding ester derivatives **6a,b**. The ^{13}C-NMR and ^{1}H-NMR spectra of compounds **6a,b** were consistent with formed structures. ^{1}H-NMR spectrum of derivative **6b** as a model displayed characteristic bands for the ethyl group at 1.35–1.38 (triplet signal for CH$_2$C**H**$_3$) and 4.32–4.35 (quartet signal for C**H**$_2$CH$_3$) in addition to characteristic singlet signals for C**H**=CH$_2$ and N**H** at 5.98 and 10.64, respectively. Reaction of ester **6b** with hydrazine hydrate afforded the corresponding hydrazide derivative **7**, which showed the disappearance of characteristic bands for ethyl ester and presence of NH$_2$, NH and hydrazide carbonyl bands, in its IR spectrum. Cyclization of acid hydrazide **7** with carbon disulfide, acetic anhydride and/or acetyl acetone afforded the corresponding oxadiazole-5-thiol **8**, 5-methyloxadiazole **9** and/or dimethylpyrazole derivative **10**, respectively (Scheme 1). IR and ^{1}H-NMR spectra for compounds **8**, **9** and **10** exhibited the disappearance of hydrazide characteristic bands. In addition, ^{1}H-NMR spectrum for compound **10** presents two singlet signals at 1.99 and 2.19 for two CH$_3$ moieties of the pyrazole group. Moreover, ^{13}C-NMR is consistent with the formed structure.

Conversely, reaction of 5-iodoanthranilic acid (**2**) with benzyl bromide afforded the corresponding *N*-benzyl derivative (**11**).[40] Fusion of 5-iodo-*N*-benzylanthranilic acid (**11**) with urea afforded 6-iodo-1-benzylquinazoline-2,4(1*H*,3*H*)-dione (**12**).[40] *In situ*

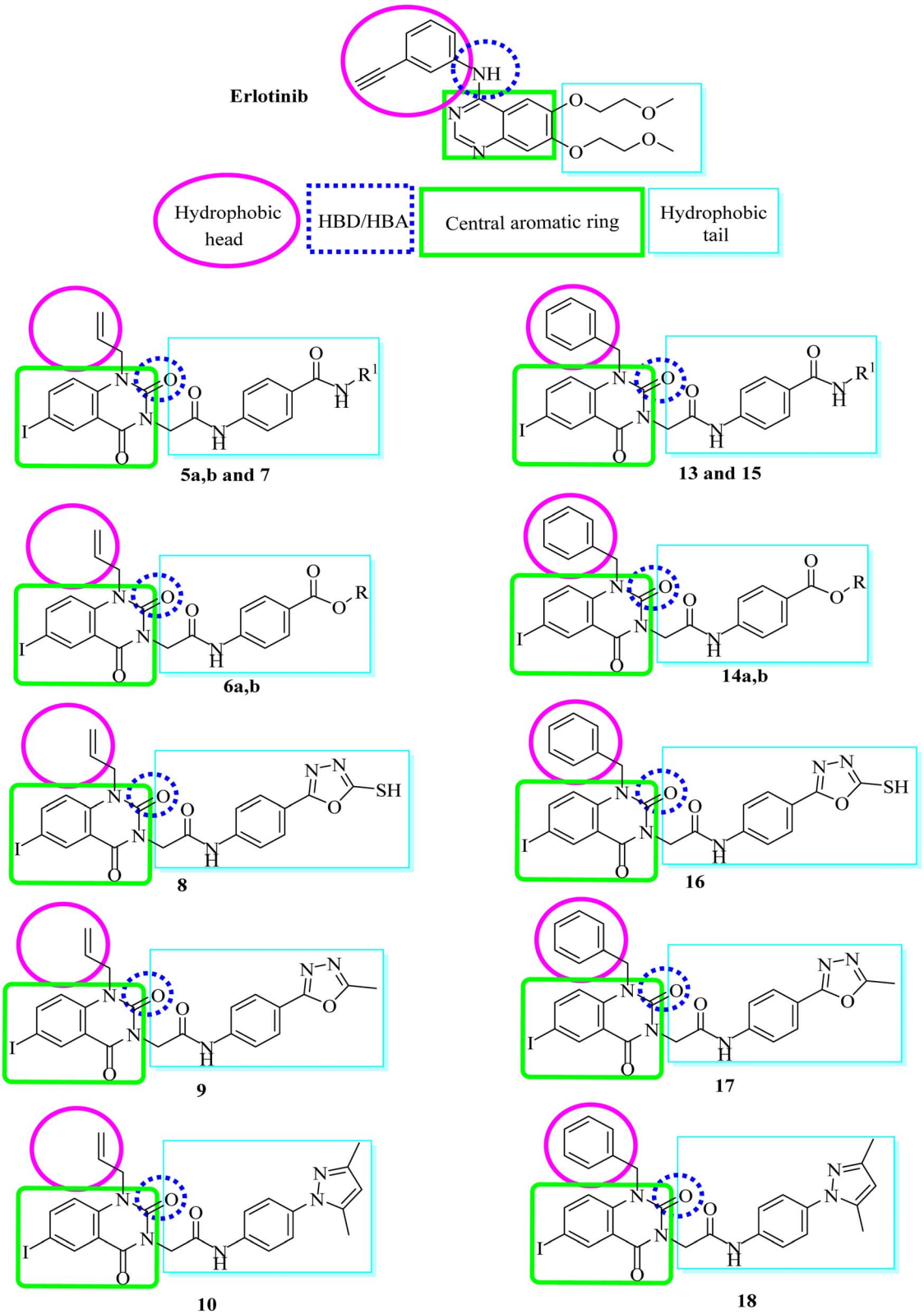

Fig. 3 Basic structural features of EGFR inhibitors.

reaction of 6-iodo-1-benzylquinazoline-2,4(1*H*,3*H*)-dione (**12**) with chloroacetamide **IIIa** afforded the corresponding benzamide derivative **13**. ^{1}H-NMR spectrum of derivative **13** revealed characteristic bands for the new *N*-benzyl group at 5.43 for NCH_2. Additionally, it showed a signal for $NHCH_3$ at 3.06. Moreover, reaction of 6-iodo-1-benzylquinazoline-2,4(1*H*,3*H*)-

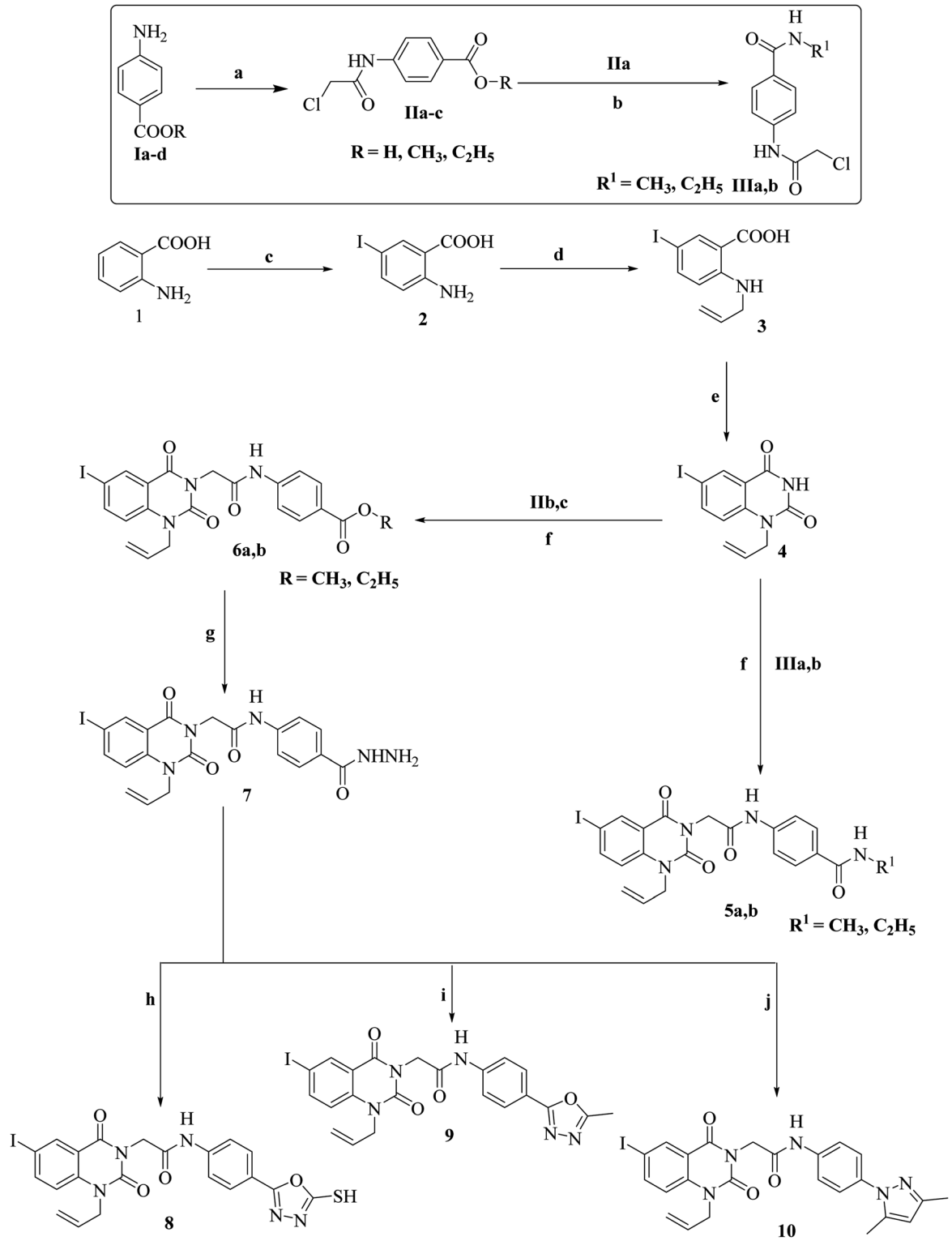

Scheme 1 Synthetic route for compounds **5a,b–10**. Reaction condition and yield: (a) $ClCH_2COCl/DMF/K_2CO_3$, 0–5 °C, 1 h, 85%; (b) ECF/TEA/DMF/NH_2-R^1, 0–5 °C, 1 h, 80–82%; (c) I_2/KOH/H_2O/stirring RT, overnight, 87%; (d) allyl bromide/K_2CO_3/ethanol/reflux, 6 h, 84%; (e) NH_2CONH_2/fusion/1 h, 85%; (f) acetone/ K_2CO_3/reflex, 12 h, 72–76%; (g) NH_2NH_2/ethanol/reflux 6 h, 80%; (h) CS_2/KOH/H_2O/ethanol/reflux/24 h, 76%; (i) AC_2O/reflux/3 h, 78%; (j) acetylacetone/dioxane/TEA/reflux, 4 h, 72%.

dione (**12**) with the appropriate chloroacetamide **IIb,c** afforded corresponding ester derivatives **14a,b.** ^{13}C-NMR and ^{1}H-NMR spectra of compounds **14a,b** were consistent with the formed structures. ^{1}H-NMR spectrum of derivative **14b** as a model displayed characteristic bands for the ethyl group at 1.26–1.29 (triplet signal for CH_2CH_3) and 4.24–4.27 (quartet signal for

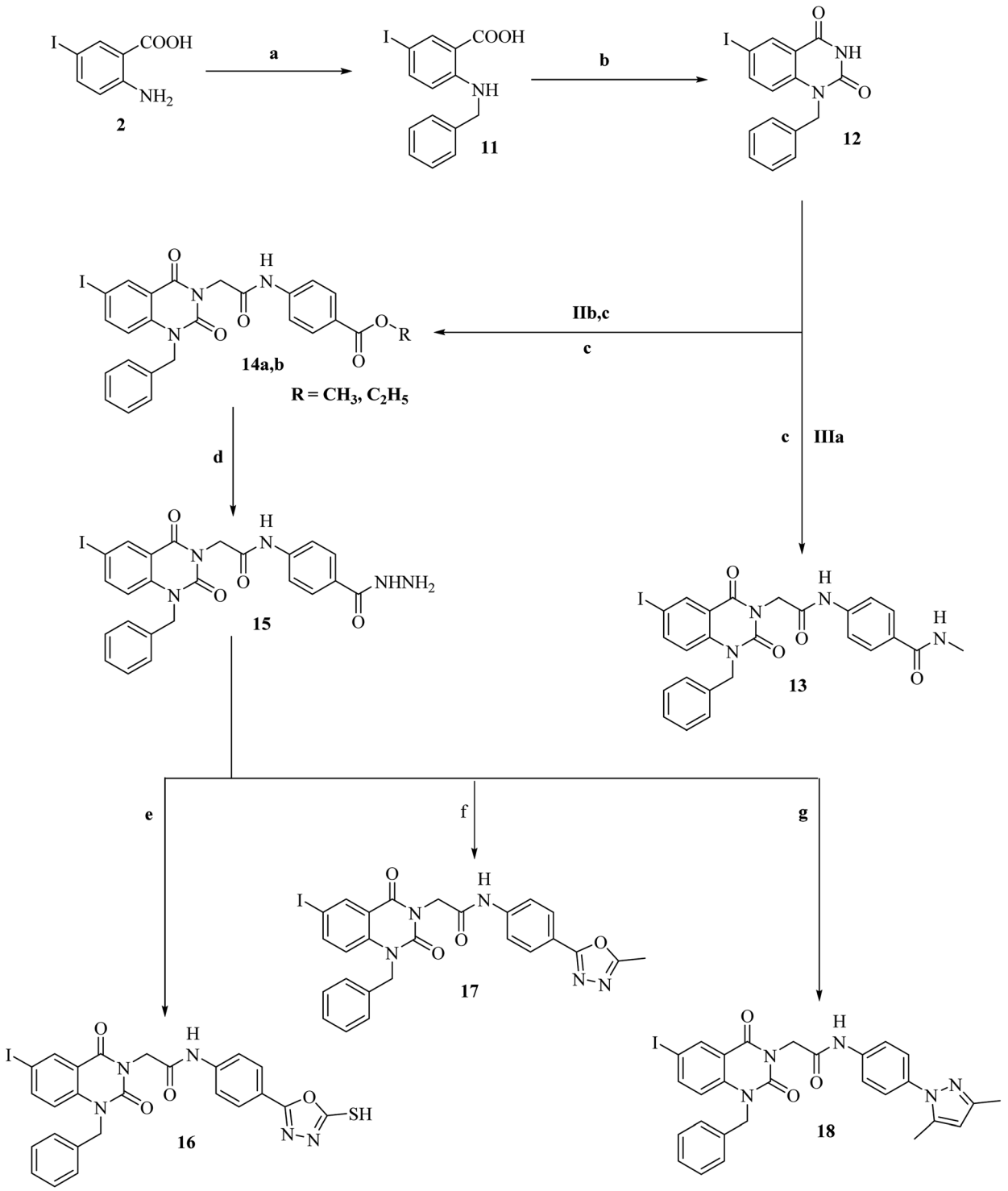

Scheme 2 Synthetic route for compounds **13a,b–18**. Reaction condition and yield: (a) benzyl bromide/K_2CO_3/ethanol/reflux, 6 h, 82%; (b) NH_2CONH_2/fusion/1 h, 85%; (c) acetone/K_2CO_3/reflex, 12 h, 70–75%; (d) NH_2NH_2/ethanol/reflux 6 h, 80%; (e) CS_2/KOH/H_2O/ethanol/reflux/24 h, 76%; (f) AC_2O/reflux/3 h, 78%; (g) acetylacetone/dioxane/TEA/reflux, 4 h, 72%.

CH_2CH_3) in addition to characteristic singlet signals for CH_2CO, NCH_2 and NH at 4.84, 5.38 and 10.67, respectively. Reaction of ester **14b** with hydrazine hydrate afforded the corresponding hydrazide derivative **15**, which showed the disappearance of the characteristic bands for ethyl ester and presence of NH_2, NH and hydrazide carbonyl bands, in its IR spectrum. Cyclization of acid hydrazide **14** with carbon disulfide, acetic anhydride and/or acetyl acetone afforded the corresponding oxadiazole-5-thiol **16**, 5-methyloxadiazole **17** and/or dimethylpyrazole derivative **18**, respectively (Scheme 2). IR and ^{1}H-NMR spectra for

compounds **8**, **9** and **10** exhibited the disappearance of hydrazide characteristic bands. In addition, ^{1}H-NMR spectrum for compound **18** presents two singlet signals at 2.17 and 2.53 for two CH_3 moieties of the pyrazole group. Additionally, ^{13}C-NMR is consistent with the formed structure.

2.2. Docking studies

For molecular docking investigations, Molsoft software was used. The PDB IDs for EGFR-TK wild-type and mutated one, $EGFR^{WT}$ (PDB: 4HJO)[41] and $EGFR^{T790M}$ (PDB ID 3W2O),[38] were used in each experiment, respectively.

2.2.1. Docking studies as $EGFR^{WT}$ inhibitors. The standard **erlotinib** showed binding energy = −92.64 kcal mol^{-1}. It made two hydrogen bonds with Cys773 (2.95 Å) and Met769 (2.00 Å). The hydrophobic region I formed by Val702, Asp831, Lys721, Ile765, Thr766, Ala719 and Thr830 was occupied by the 3-ethynylphenyl head. Moreover, 2-methoxyethoxy side chains engaged the hydrophobic furrow II created by Leu694, Asp776, Cys773, Leu820, Gly772, Phe771, Met769 and Pro770 (Fig. 4).

Compound **18** presented undistinguishable binding features from those of **erlotinib**. It displayed a binding energy of −109.97 kcal mol^{-1} and three H-bonds with Asp831 (2.47 Å), Thr766 (2.96 Å) and Met769 (2.95 Å) (Fig. 5).

Compound **17** presented nearly undistinguishable docking from that of **erlotinib** and **18**. It exhibited a binding energy of −108.87 kcal mol^{-1} (Table 1) and four H-bonds with Asp831 (2.48 Å), Thr766 (2.96 Å), Met769 (1.70 Å) and Gly772 (2.96 Å) (Fig. 6). Moreover, compound **14b** exhibited a binding energy of −108.27 kcal mol^{-1} and formed three H-bonds with Asp831 (2.46 Å), Thr766 (2.66 Å) and Met769 (2.54 Å) (Fig. 7).

2.2.2. Docking results for $EGFR^{T790M}$ inhibition studies. **Erlotinib** presented binding energy = −82.77 kcal mol^{-1} and

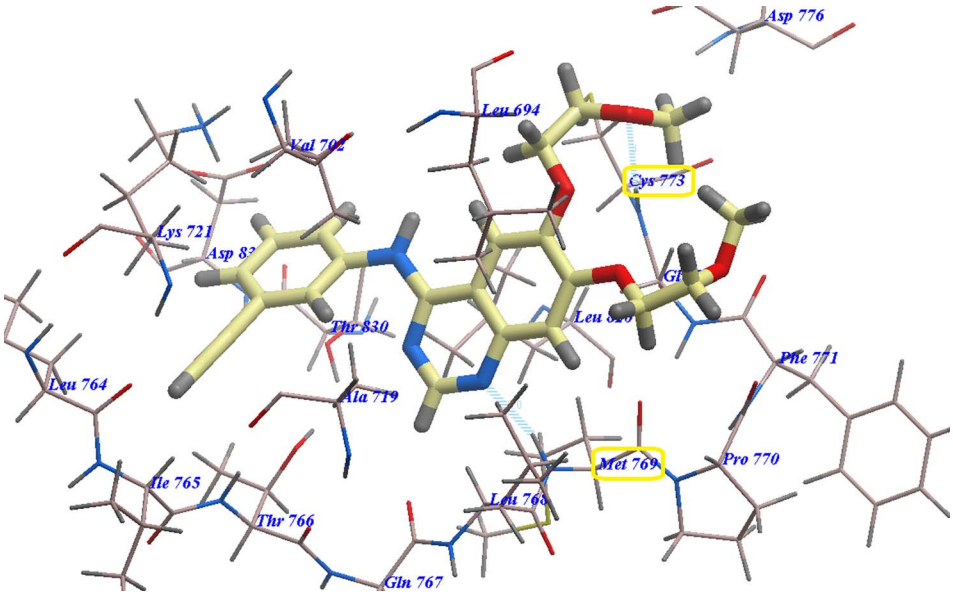

Fig. 4 **Erlotinib** expected binding mode with 4HJO.

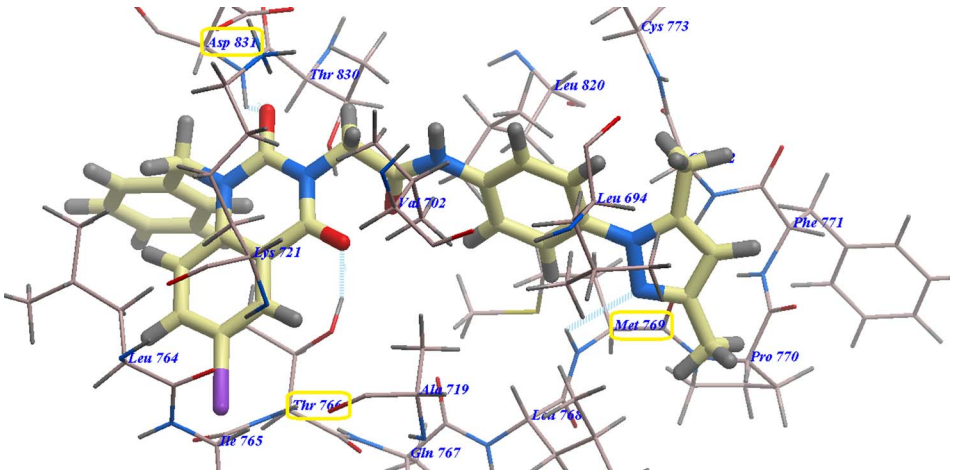

Fig. 5 **18** expected binding mode with 4HJO.

Table 1 Calculated free energy (Δ*G*) of ligands binding with EGFR^{WT}

Compound	Δ*G* [kcal mol^{-1}]	Compound	Δ*G* [kcal mol^{-1}]
5a	−89.65	**13**	−98.86
5b	−95.87	**14a**	−98.84
6a	−91.11	**14b**	−108.27
6b	−99.13	**15**	−97.98
7	−88.36	**16**	−108.12
8	−97.98	**17**	−108.87
9	−99.12	**18**	−109.97
10	−102.09	**Erlotinib**	−92.64

four H-bonds with Cys797 (2.05 Å), Val726 (2.97 Å), Met793 (1.82 Å) and Thr854 (2.99 Å). The hydrophobic region I formed by Phe723, Ile759, Glu762, Met790, Glu791, Thr854, Asp855, Val726 and Leu777 was occupied by the 3-ethynylphenyl head. Moreover, the 2-methoxyethoxy tail engaged the hydrophobic furrow II created by Leu718, Met793, Pro794, Leu844 and Val845 (Fig. 8).

Compound **17** exhibited a nearly undistinguishable pattern from that of **erlotinib**. It demonstrated a binding energy of −95.80 kcal mol^{-1} (Table 2) and five H-bonds with Thr854 (2.95 Å), Val726 (2.96 Å), Cys797 (2.96 Å), Met793 (2.60 Å) and Phe795 (2.95 Å) (Fig. 9).

Compounds **18** and **14b** presented identical docking patterns to those of **erlotinib** and **17**, with affinities of −95.07 kcal mol^{-1} (forming 4 H-bonds) (Fig. 10) and −94.74 kcal mol^{-1} (forming 4 H-bonds) (Fig. 11), respectively.

2.3. Biological evaluation

2.3.1. Measuring the cytotoxic activity. The MTT assay, reported by Mosmann,[42,43] was used for assessment of new iodoquinazoline compounds **5a–c** to **18** against A549, HCT116, MCF-7 and HepG2 (Table 3). Compounds **18**, **17** and **14b** showed the highest anticancer effects with IC_{50} = 5.25, 6.46, 5.68 and 5.24 μM, 5.55, 6.85, 5.40 and 5.11 μM and 5.86, 7.03, 6.15 and 5.77 μM against the HepG2, MCF-7, HCT116 and A549 cell lines, respectively.

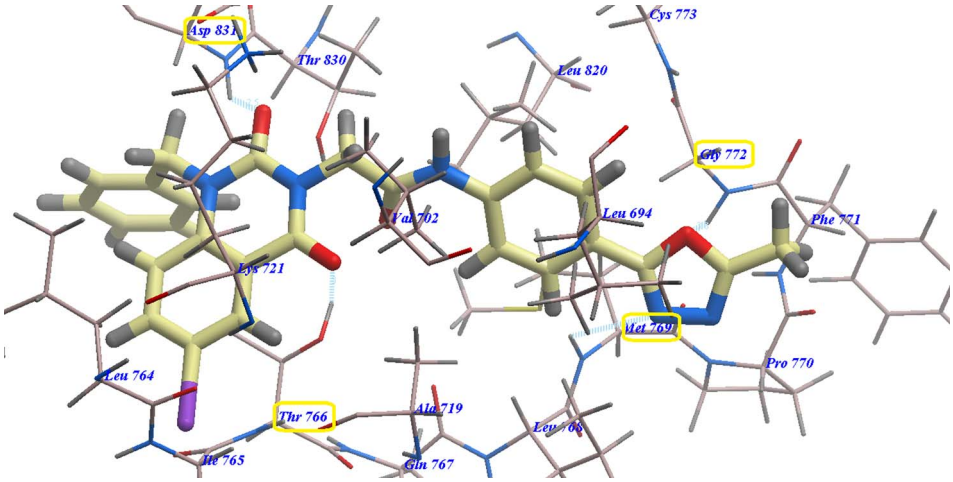

Fig. 6 **17** expected binding mode with 4HJO.

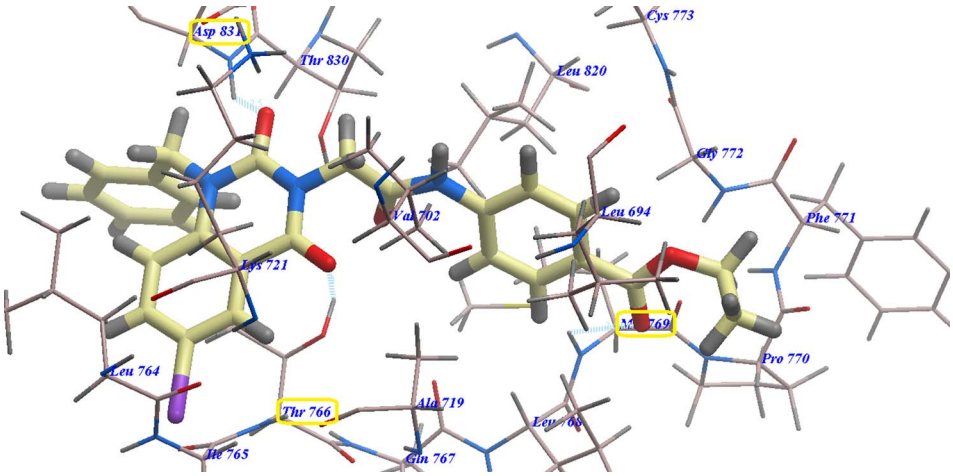

Fig. 7 **14b** expected binding mode with 4HJO.

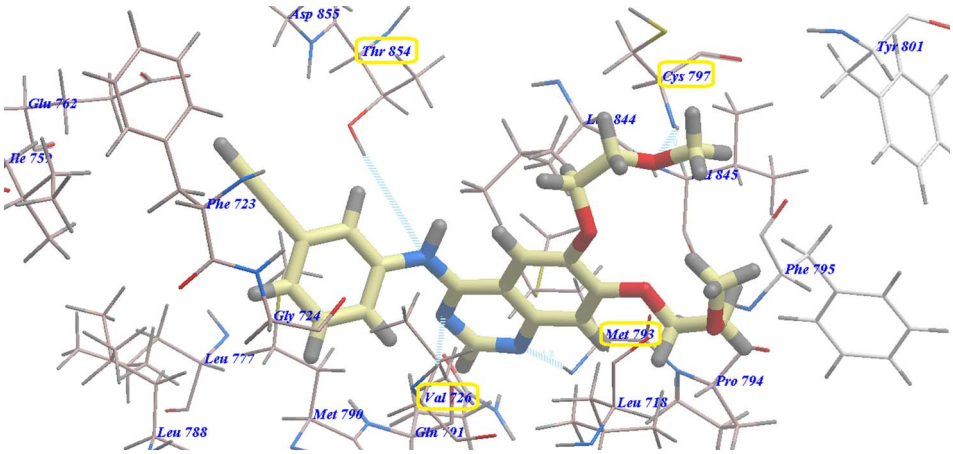

Fig. 8 Docking results for **erlotinib** with 3W2O.

Table 2 Calculated free energy (ΔG) of synthesized compounds binding with $EGFR^{T790M}$

Compound	ΔG [kcal mol^{-1}]	Compound	ΔG [kcal mol^{-1}]
5a	−78.53	**13**	−93.30
5b	−82.40	**14a**	−86.89
6a	−82.32	**14b**	−94.74
6b	−84.74	**15**	−82.06
7	−70.72	**16**	−91.70
8	−84.27	**17**	−95.80
9	−86.18	**18**	−95.07
10	−85.42	**Erlotinib**	−82.77

Regarding HepG2, compounds **10**, **13**, **14a**, **15** and **16** exhibited very good anticancer effects with IC_{50} ranging from 6.54 to 9.50 μM. Derivatives **5b**, **6a**, **6b**, **8** and **9** with IC_{50} ranging from 11.00 to 13.03 μM presented good cytotoxicity. In contrast, derivatives **5a** and **7** displayed moderate anticancer effects with IC_{50} = 15.00 and 16.50 μM, respectively.

Concerning MCF-7, compounds **10**, **13**, **14a**, **15** and **16** exhibited very good anticancer effects with IC_{50} ranging from 7.36 to 8.80 μM. Derivatives **5a**, **5b**, **6a**, **6b**, **8** and **9** with IC_{50} ranging from 10.44 to 13.44 μM presented good cytotoxicity. Conversely, derivative **7** displayed moderate anticancer effects with IC_{50} = 15.20 μM.

Derivatives **6b**, **8**, **9**, **10**, **13**, **14a**, **15** and **16** exhibited very good anticancer effects with IC_{50} ranging from 6.67 to 9.79 μM against HCT116. Derivatives **5a**, **5b**, and **6a** with IC_{50} = 13.44, 11.00 and 12.05 μM displayed good cytotoxicity. Conversely, derivative **7** revealed moderate anticancer effect with IC_{50} = 15.15 μM.

Derivatives **5b**, **6b**, **8**, **9**, **10**, **13**, **14a**, **15** and **16** exhibited very good anticancer effects with IC_{50} ranging from 6.20 to 9.50 μM against A549. Derivatives **5a**, **6a** and **7** with IC_{50} = 10.60, 10.40 and 12.20 μM showed good cytotoxicity.

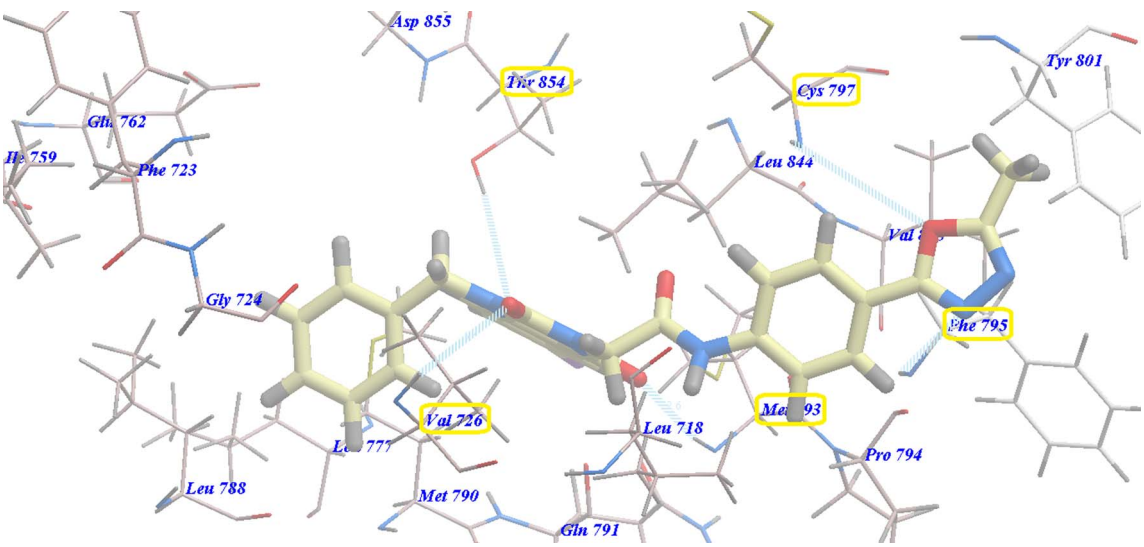

Fig. 9 Docking of **17** in the active site of 3W2O.

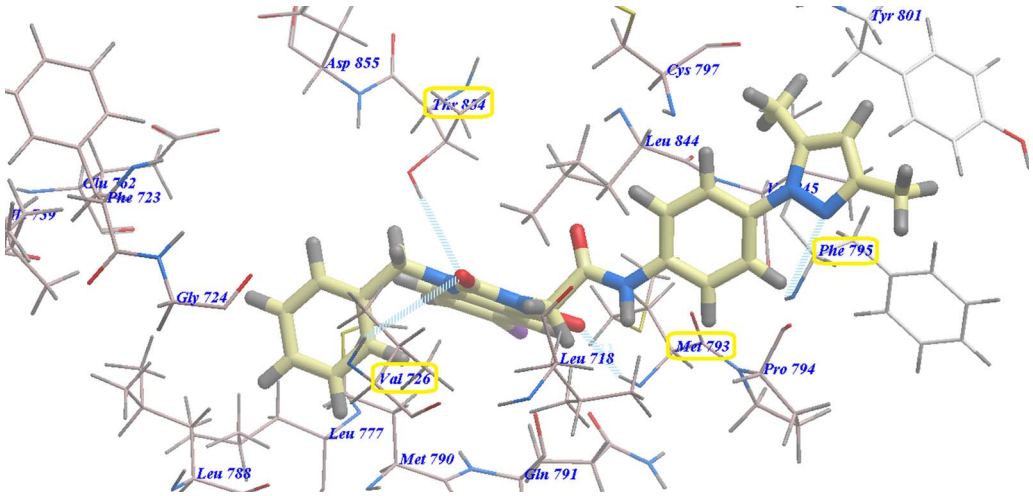

Fig. 10 Docking of **18** in the active site of 3W2O.

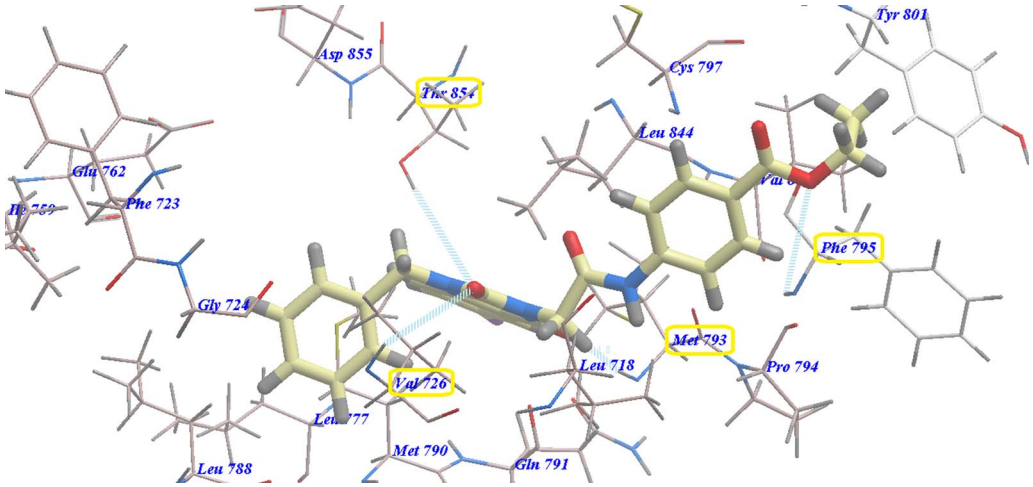

Fig. 11 Docking of **14b** in the active site of 3W2O.

2.3.1.1. Selectivity index (SI). To evaluate toxicity induced by our iodoquinazoline derivatives, the eight highly effective derivatives **10**, **13**, **14a**, **14b**, **15**, **16**, **17** and **18** were tested against VERO normal cells. All results revealed that each compound possessed low toxicity against VERO normal cells with IC_{50} ranging from 43.44 to 52.11 μM. One criterion for an anticancer drug to be good is that it should not affect non-cancer cells. A molecule could be considered as highly selective for cancer cells if it presents SI value ≥5. A molecule with moderate selectivity presents SI value >2, while low selectivity is considered if the SI is lower than 2.[43] In this study, derivatives **10**, **13**, **14a**, **14b**, **15**, **16**, **17** and **18** are correspondingly 5.91-, 5.86-, 5.58-, 8.39-, 5.49-, 6.69-, 8.31- and 8.67-fold more toxic against HepG2 than VERO cells. More, derivatives **10**, **13**, **14a**, **14b**, **15**, **16**, **17** and **18** are correspondingly 5.53-, 5.68-, 6.01-, 6.99-, 5.92-, 5.95-, 6.73- and 7.04-fold more toxic in MCF-7 than in VERO cells. Furthermore, structures **10**, **13**, **14a**, **14b**, **15**, **16**, **17** and **18** have respectively 6.24-, 6.37-, 5.91-, 7.99-, 5.82-, 6.56-, 7.69- and 8.43-fold grander lethalness in HCT116 than in VERO cells. Additionally, products **10**, **13**, **14a**, **14b**, **15**, **16**, **17** and **18** have respectively 6.30-, 6.60-, 6.38-, 8.52-, 6.37-, 7.06-, 8.63- and 8.90-fold more toxicity in A549 than in VERO cells. All compounds displayed high selectivity against tested cancer cell lines with SI values >5 which revealed a high selectivity against the tested cancer cell lines.

2.3.2. *In vitro* $EGFR^{WT}$ kinase inhibitory assay. Additionally, all derivatives were assessed for their capability to inhibit $EGFR^{WT}$.[44] Compound **17** exhibited the same inhibitory activity as erlotinib. Compounds **10**, **13**, **14b**, **16** and **18** excellently inhibited $EGFR^{WT}$ activity with IC_{50} ranging from 0.17 to 0.50 μM. Candidates **5b**, **6b**, **8**, **9**, **14a** and **15** significantly inhibited $EGFR^{WT}$ at IC_{50} range of 0.60–1.00 μM. Also, compounds **6a**, **5a** and **7** moderately inhibited $EGFR^{WT}$ at IC_{50} = 1.32, 1.15 and 1.50 μM, respectively (Table 3).

2.3.3. *In vitro* $EGFR^{T790M}$ kinase inhibitory assay. All compounds were also assessed for their $EGFR^{T790M}$ kinase

Table 3 $EGFR^{WT}$ and $EGFR^{T790M}$ kinase assays and *in vitro* cytotoxic effects against the HepG2, MCF-7, HCT116, A549 and VERO cell lines

	IC_{50}[a] (μM)						
Compound	HepG2	MCF-7	HCT116	A549	VERO	$EGFR^{WT}$	$EGFR^{T790M}$
5a	15.00 ± 1.5	13.22 ± 1.0	13.44 ± 1.5	10.60 ± 1.5	NT[b]	1.32 ± 0.25	1.62 ± 0.20
5b	12.53 ± 1.0	11.26 ± 1.1	11.00 ± 1.3	9.50 ± 1.5	NT[b]	1.00 ± 0.15	1.33 ± 0.10
6a	13.03 ± 1.4	12.25 ± 1.7	12.05 ± 1.5	10.40 ± 1.5	NT[b]	1.15 ± 0.25	1.54 ± 0.50
6b	11.58 ± 1.8	10.95 ± 1.6	9.79 ± 1.8	9.39 ± 1.5	NT[b]	0.95 ± 0.35	1.12 ± 0.50
7	16.50 ± 1.6	15.20 ± 1.9	15.15 ± 1.7	12.20 ± 1.5	NT[b]	1.50 ± 0.15	1.90 ± 0.50
8	11.15 ± 1.9	10.77 ± 1.8	9.31 ± 1.8	9.00 ± 1.5	NT[b]	0.88 ± 0.35	0.96 ± 0.50
9	11.00 ± 1.4	10.44 ± 1.7	8.62 ± 1.5	7.06 ± 1.5	NT[b]	0.80 ± 0.25	0.89 ± 0.50
10	7.35 ± 1.0	7.85 ± 0.9	6.96 ± 1.1	6.90 ± 1.5	43.44 ± 0.31	0.38 ± 0.35	0.54 ± 0.50
13	8.00 ± 1.3	8.25 ± 1.1	7.36 ± 1.1	7.10 ± 1.1	46.88 ± 0.43	0.50 ± 0.15	0.61 ± 0.10
14a	9.00 ± 1.2	8.35 ± 1.5	8.50 ± 1.1	7.87 ± 1.1	50.22 ± 0.31	0.60 ± 0.35	0.75 ± 0.50
14b	5.86 ± 1.0	7.03 ± 1.1	6.15 ± 1.5	5.77 ± 1.3	49.14 ± 0.32	0.25 ± 0.35	0.36 ± 0.10
15	9.50 ± 1.0	8.80 ± 1.0	8.95 ± 1.0	8.18 ± 1.0	52.11 ± 0.31	0.65 ± 0.15	0.80 ± 0.10
16	6.54 ± 1.0	7.36 ± 1.0	6.67 ± 1.0	6.20 ± 1.0	43.78 ± 0.42	0.33 ± 0.25	0.43 ± 0.10
17	5.55 ± 0.7	6.85 ± 0.9	5.40 ± 1.5	5.11 ± 1.1	46.11 ± 0.31	0.15 ± 0.35	0.30 ± 0.50
18	5.25 ± 0.7	6.46 ± 0.9	5.68 ± 1.5	5.24 ± 1.1	45.50 ± 0.31	0.17 ± 0.35	0.25 ± 0.50
Erlotinib	7.73 ± 0.67	13.91 ± 1.3	8.20 ± 0.34	5.49 ± 0.45	NT[b]	0.15 ± 0.02	0.24 ± 0.22

[a] IC_{50} values are the mean ± SD of three separate experiments. [b] NT: not tested.

inhibitory activities.[44,45] Compounds **18**, **17**, **14b** and **16** excellently inhibited $EGFR^{T790M}$ activity with IC_{50} = 0.25, 0.30, 0.36 and 0.40 μM respectively. Candidates **8**, **9**, **10**, **13**, **14a** and **15** significantly inhibited $EGFR^{T790M}$ at IC_{50} range of 0.54–0.96 μM. Also, compounds **6b** and **5b** moderately inhibited $EGFR^{T790M}$ at IC_{50} = 1.12 and 1.33 μM respectively. The least inhibitory effect against VEGFR-2 was demonstrated by compounds **5a** and **7** (Table 3). As planned, compounds **18**, **17** and **14b** showed excellent dual $EGFR^{WT}$/$EGFR^{T790M}$ inhibitory activities.

2.3.4. Structure activity relationship (SAR). The A549 cell line was the most sensitive to the effect of our novel compounds. Generally, compounds **13**, **14a,b**, **15**, **16**, **17** and **18** with 1-benzyl substitutions displayed higher anticancer activities than compounds **5a,b**, **6a,b**, **7**, **8**, **9** and **10** with 1-allyl substitutions.

The molecular modeling and biological data obtained suggested that the high activities of benzyl derivatives may be due to that the benzyl moiety was expected to occupy the hydrophobic region I more than the allyl one. In addition, the carbonyl groups of quinazoline scaffold formed different H-bonds with amino acid residues in the linker and/or adenine binding sites. Moreover, the long hydrophobic side chains attached to the quinazoline scaffold at position-3 occupied the hydrophobic region II. All the mentioned structural elements are necessary for higher activities and/or binding with the active sites of EGFR receptors.

Based on the structures of synthesized derivatives and data in Table 3, we can divide the tested compounds into two groups.

Compounds **5a,b**, **6a,b**, and **7** with 1-allyl substitutions and amide, ester and hydrazide, respectively, belong to the first group. Moreover, this group contains compounds **13**, **14a,b** and **15** with 1-benzyl substitutions and amide, ester and hydrazide respectively.

Compound **14b** with a more hydrophobic ethyl ester side chain exhibited higher anticancer activities than compound **13** with methyl amide and compound **14a** with methyl ester side chains against the four tested cell lines. Compound **15** with a hydrazide side chain showed the lowest activities among this group.

In the same manner, compound **6b** with a more hydrophobic ethyl ester side chain exhibited higher anticancer activities than compound **5b** with ethyl amide, compound **6a** with methyl ester and compound **5a** with methyl amide side chains against the four tested cell lines. Compound **7** with a hydrazide side chain showed the lowest activities among this group.

The second group consists of compounds **16**, **17** and **18** with 1-benzyl substitutions and heteroaromatic distal hydrophobic side chains. Additionally, compounds **8**, **9** and **10** with 1-allyl substitutions and heteroaromatic distal hydrophobic side chains belong to this group.

Compound **18** with a highly lipophilic electron-donating 3,5-dimethylpyrazole moiety showed stronger activity than derivative **17** with 5-methyloxadiazole, and compound **16** with 5-mercapto-oxadiazole moiety against MCF-7 and HepG2. While against A549 and HCT116, the order of activity is **17** > **18** > **16**.

Conversely, derivative **10** with a highly lipophilic electron-donating 3,5-dimethylpyrazole moiety showed stronger activity than derivative **9** with 5-methyloxadiazole and compound **8** with 5-mercapto-oxadiazole moiety against the four MCF-7, HepG2, A549 and HCT116 cell lines.

2.4. ADMET; *in silico* studies profile

In silico prediction of the highly active derivatives **14b**, **17** and **18** was calculated for their physicochemical character evaluation and the proposed ADMET profile. It was predicted using pkCSM descriptor algorithm procedures[46] and matched to the rule of five described by Lipinski.[47] Good absorption properties were expected for the molecules that follow at least three of the following rules: (i) no more than five hydrogen bond donors, (ii)

no more than 10 hydrogen bond acceptors, (iii) molecular weight less than 500, (iv) not more than 5 for log *P*. In the current study, our new compounds **14b**, **17** and **18** violate the molecular weight rule, while the standard anticancer agent erlotinib does not violate any rule.

As a result of obtaining data from Table 4, we can assume that compounds **14b**, **17** and **18** have very good GIT absorption in humans (92.177 to 99.768), which indicates that they more easily cross different biological membranes.[48] Thus, they may show a significantly high bioavailability through GIT. Concerning CNS penetrability, our prepared compounds can reach the CNS, with CNS permeability values of −2.299 to −1.962, comparable to that of erlotinib (−3.216).

It is well known that CYP3A4, a major drug-metabolizing enzyme, could be inhibited by erlotinib and by our derivatives **14b**, **17** and **18**. Elimination was expected depending on the total clearance which is a considerable factor in deciding dose intervals. The data showed that erlotinib exhibited higher clearance rates compared with our new compounds which demonstrated low clearance values. Thus, erlotinib could be eliminated faster, and as a result, supposed to have shorter dosing intervals. Unlike erlotinib, the prepared compounds exhibited low clearance rates, which signifies a long duration of action and extended dosing intervals. Toxicity is the final ADMET profile factor studied. As presented in Table 4, erlotinib and the novel compounds **14b**, **17** and **18** shared the drawback of unwanted hepatotoxic actions. Erlotinib, **17** and **18** demonstrated high maximum tolerated dose. In contrast, **14b** demonstrated lower maximum tolerated doses which involve the advantage of the broad therapeutic index of erlotinib, **17** and **18**. Lastly, the oral acute toxic doses of the novel compounds **14b**, **17** and **18** are higher than that of erlotinib. Moreover, the oral chronic toxic doses of the novel compounds **14b** and **17** are nearly equal to that of erlotinib but higher than that of **18**.

Table 4 Data for the most effective compounds, sorafenib and erlotinib; ADMET profile

Parameter	14b	17	18	Erlotinib
Physicochemical properties				
Molecular weight	583.382	593.381	605.436	393.443
Log *P*	3.6315	3.81322	4.25734	3.4051
Rotatable bonds	7	6	6	10
Acceptors	7	8	7	7
Donors	1	1	1	1
Surface area	213.847	218.102	225.872	169.532
Absorption				
Water solubility	−5.318	−4.679	−5.204	−4.736
Human intest. absorption	92.177	92.423	99.768	94.58
Substrate for *P*-glycoprotein	Yes	Yes	Yes	No
Inhibitor of *P*-glycoprotein I	Yes	Yes	Yes	Yes
Inhibitor of *P*-glycoprotein II	Yes	Yes	Yes	Yes
Distribution				
Permeability through BBB	−1.106	−1.338	−1.084	−0.745
Permeability to CNS	−2.299	−2.225	−1.962	−3.216
Metabolism				
CYP2D6 substrate	No	No	No	No
CYP3A4 substrate	Yes	Yes	Yes	Yes
Inhibition of CYP1A2	No	No	No	Yes
Inhibition of CYP2C19	Yes	Yes	Yes	Yes
Inhibition of CYP2C9	Yes	Yes	Yes	Yes
Inhibition of CYP2D6	No	No	No	No
Inhibition of CYP3A4	Yes	Yes	Yes	Yes
Excretion				
Clearance	−0.482	−0.556	−0.587	0.702
Toxicity				
Human max. tolerated dose	0.37	0.701	0.559	0.839
Acute toxic activity (LD_{50})	2.683	2.816	2.621	2.393
Chronic toxic activity (LOAEL)	1.366	1.32	0.862	1.37
Hepatotoxic effect	Yes	Yes	Yes	Yes

3. Conclusion

Fifteen new iodoquinazoline derivatives bearing different side chain moieties were designed and synthesized as dual $EGFR^{WT}$/$EGFR^{T790M}$ inhibitors. The cytotoxic activities of the new compounds were screened *in vitro* against four different cancer cell lines (HepG2, MCF-7, HCT116 and A549) using an MTT assay. Their ability to bind with $EGFR^{WT}$ and $EGFR^{T790M}$ receptors was examined by molecular modeling. Compounds **18**, **17** and **14b** showed the highest anticancer effects with IC_{50} = 5.25, 6.46, 5.68 and 5.24 μM, 5.55, 6.85, 5.40 and 5.11 μM and 5.86, 7.03, 6.15 and 5.77 μM against the HepG2, MCF-7, HCT116 and A549 cell lines, respectively. Compounds **10**, **13**, **14a**, **15** and **16** exhibited very good anticancer effects against the tested cancer cell lines. The eight highly effective derivatives **10**, **13**, **14a**, **14b**, **15**, **16**, **17** and **18** were examined against VERO normal cell line. These compounds possessed low toxicity against VERO normal cells with IC_{50} ranging from 43.44 to 52.11 μM. Additionally, all derivatives were evaluated for their ability as dual inhibitors of $EGFR^{WT}$ and $EGFR^{T790M}$. The evaluated candidates showed excellent-to-low inhibitory activities.

Compound **17** exhibited the same inhibitory activity as erlotinib. Compounds **10**, **13**, **14b**, **16** and **18** remarkably inhibited $EGFR^{WT}$ activity with IC_{50} ranging from 0.17 to 0.50 μM. Candidates **5b**, **6b**, **8**, **9**, **14a** and **15** significantly inhibited $EGFR^{WT}$ at an IC_{50} range of 0.60–1.00 μM. Moreover, compounds **18**, **17**, **14b** and **16** excellently inhibited $EGFR^{T790M}$ activity with IC_{50} = 0.25, 0.30, 0.36 and 0.40 μM respectively. Candidates **8**, **9**, **10**, **13**, **14a** and **15** significantly inhibited $EGFR^{T790M}$ at an IC_{50} range of 0.54–0.96 μM. Further, an ADMET study was conducted *in silico* for three best-performing compounds **14b**, **17** and **18** in comparison with erlotinib. Our derivatives may be promising as prototypes for design, optimization, adaptation and investigation to construct further powerful selective dual $EGFR^{WT}$/$EGFR^{T790M}$ inhibitors with higher antitumor activities.

4. Experimental

4.1. Chemistry

^{1}H-NMR spectra were recorded with a Bruker 400 MHz NMR spectrophotometer at Microanalytical Center, Ain Shams

University and/or a Mercury 300 MHz NMR spectrophotometer at Faculty of Science, Cairo University. ^{13}C-NMR spectra were recorded with a Bruker 100 MHz NMR spectrophotometer at Microanalytical Unit, Faculty of Pharmacy, Cairo University.

Alkyl 4-(2-chloroacetamido)benzoate (**IIa–c**), 4-(2-chloroacetamido)-*N*-alkylbenzamide (**IIIa,b**), 5-iodoanthranilic acid (**2**), 5-iodo-*N*-allylanthranilic acid (**3**), 6-iodo-1-allylquinazoline-2,4(1*H*,3*H*)-dione (**4**), 5-iodo-*N*-benzylanthranilic acid (**11**), and 6-iodo-1-benzylquinazoline-2,4(1*H*,3*H*)-dione (**12**) were synthesized according to reported procedures.[38–40]

4.1.1. 4-{2-[1-Allyl-6-iodo-2,4-dioxo-1,4-dihydroquinazolin-3(2*H*)-yl]acetamido}-*N*-alkylbenzamide (5a,b)

4.1.1.1. General method. A mixture of equimolar quantities of 6-iodo-1-allylquinazoline-2,4(1*H*,3*H*)-dione (**4**) (3.28 g, 0.01 mol) and appropriate 4-(2-chloroacetamido)-*N*-alkylbenzamide (**IIIa,b**) (0.01 mol) in dry acetone (50 mL) was heated under reflux for 12 h in the presence of K_2CO_3 (1.38 g, 0.01 mol). The reaction mixture was filtered off while hot. The precipitated solids were filtered, dried and crystallized from ethanol to give corresponding target compounds **5a,b**.

*4.1.1.2. 4-{2-[1-Allyl-6-iodo-2,4-dioxo-1,4-dihydroquinazolin-3(2H)-yl]acetamido}-N-methylbenzamide (**5a**).* Yield, 75%; m.p. 290–2 °C; $IR_{\nu max}$ (cm^{-1}): 3280, 3250 (2NH), 1694, and 1655 (4C=O); ^{1}H-NMR (400 MHz, DMSO-d_6): 3.82 (s, 3H, NHC**H**$_3$), 4.78–4.82 (m, 2CH$_2$, C**H**$_2$CO & C**H**$_2$CH), 5.13–5.21 (m, 2H, C**H**$_2$=CH), 5.83–5.95 (m, 1H, C**H**=CH$_2$), 7.31–7.91 (m, 7H, 7Ar–H), 9.46 (s, 1H, **NH**CH$_3$ (D_2O exchangeable)), and 10.63 (s, 1H, NH, D_2O exchangeable); ^{13}C-NMR (100 MHz, DMSO-d_6): 14.4, 50.8, 54.1, 94.4, 105.9, 115.0 (2), 120.9, 125.6 (3), 129.1, 131.4, 133.3, 134.5, 146.6, 151.2, 154.7, 165.2, 167.1, and 168.9; anal. calcd for $C_{21}H_{19}IN_4O_4$ (m.w. 518.31): C, 48.66; H, 3.70; and N, 10.81. Found: C, 48.74; H, 3.75; and N, 10.75.

*4.1.1.3. 4-{2-[1-Allyl-6-iodo-2,4-dioxo-1,4-dihydroquinazolin-3(2H)-yl]acetamido}-N-ethylbenzamide (**5b**).* Yield, 76%; m.p. 292–4 °C; $IR_{\nu max}$ (cm^{-1}): 3308, 3180 (2NH), 1658, and 1632 (4C=O); ^{1}H-NMR (400 MHz, DMSO-d_6): 1.21–125 (t, 3H, CH$_2$C**H**$_3$), 3.82–3.88 (q, 2H, C**H**$_2$CH$_3$), 4.89 (s, 2H, CH$_2$CO), 5.10–5.18 (m, 2CH$_2$, C**H**$_2$CH & C**H**$_2$=CH), 5.88–5.92 (m, 1H, C**H**=CH$_2$), 7.23–7.98 (m, 7H, 7Ar–H), 8.95 (s, 1H, **NH**CH$_2$ (D_2O exchangeable)), and 11.57 (s, 1H, NH, D_2O exchangeable); ^{13}C-NMR (100 MHz, DMSO-d_6): 16.6, 29.7, 54.6, 58.3, 93.3, 115.0, 121.4 (2), 125.5, 127.0, 129.7 (3), 130.7, 134.2, 138.9, 143.6, 154.6, 156.3, 166.2, and 173.4; anal. calcd for $C_{21}H_{19}IN_4O_4$ (m.w. 518.31): C, 48.66; H, 3.70; and N, 10.81. Found: C, 48.55; H, 3.75; and N, 10.70.

4.1.2. Alkyl 4-{2-[1-allyl-6-iodo-2,4-dioxo-1,4-dihydroquinazolin-3(2*H*)-yl]acetamido}benzoate (6a,b)

4.1.2.1. General method. A mixture of equimolar quantities of 6-iodo-1-allylquinazoline-2,4(1*H*,3*H*)-dione (**4**) (3.28 g, 0.01 mol) and appropriate alkyl 4-(2-chloroacetamido)benzoate **IIb,c** (0.01 mol) in dry acetone (50 mL) was heated under reflux for 12 h in the presence of K_2CO_3 (1.38 g, 0.01 mol). The reaction mixture was filtered off while hot. The precipitated solids were filtered, dried and crystallized from ethanol to give corresponding target compounds **6a,b**.

*4.1.2.2. Methyl 4-{2-[1-allyl-6-iodo-2,4-dioxo-1,4-dihydroquinazolin-3(2H)-yl]acetamido}benzoate (**6a**).* Yield, 72%; m.p. 263–5 °C; $IR_{\nu max}$ (cm^{-1}): 3481 (NH), 1725, 1672, and 1653 (4C=O); ^{1}H-NMR (400 MHz, DMSO-d_6): 3.78 (s, 3H, COOC**H**$_3$), 4.75–4.78 (m, 2CH$_2$, C**H**$_2$CO & C**H**$_2$CH), 5.12–5.14 (m, 2H, C**H**$_2$=CH), 5.87–5.90 (m, 1H, C**H**=CH$_2$), 7.38–7.90 (m, 7H, 7Ar–H), and 10.65 (s, 1H, NH, D_2O exchangeable); ^{13}C-NMR (100 MHz, DMSO-d_6): 35.1, 53.4, 57.6, 95.6, 125.0 (2), 126.5, 128.3, 129.9 (3), 136.6, 137.9, 139.4, 149.0, 152.1, 155.8, 158.8, 162.9, 168.3, and 172.3; anal. calcd for $C_{21}H_{18}IN_3O_5$ (m.w. 519.30): C, 48.57; H, 3.49; and N, 8.09. Found: C, 48.55; H, 3.58; and N, 7.96.

*4.1.2.3. Ethyl 4-{2-[1-allyl-6-iodo-2,4-dioxo-1,4-dihydroquinazolin-3(2H)-yl]acetamido}benzoate (**6b**).* Yield, 75%; m.p. 256–8 °C; $IR_{\nu max}$ (cm^{-1}): 3290 (NH), 1718, 1701, 1685, and 1675 (4C=O); ^{1}H-NMR (400 MHz, DMSO-d_6): 1.35–1.38 (t, 3H, CH$_2$C**H**$_3$), 4.32–4.35 (q, 2H, C**H**$_2$CH$_3$), 4.80 (s, 2H, C**H**$_2$CO), 4.96 (d, 2H, C**H**$_2$CH), 5.22–5.29 (m, 2H, C**H**$_2$=CH), 5.90–5.98 (m, 1H, C**H**=CH$_2$), 7.19–8.25 (m, 7H, 7Ar–H), and 10.64 (s, 1H, NH, D_2O exchangeable); ^{13}C-NMR (100 MHz, DMSO-d_6): 19.2, 33.3, 48.3, 51.6, 95.7, 121.4, 122.5 (2), 124.0, 126.8, 128.4, 129.6 (3), 131.9, 136.6, 137.8, 144.3, 148.9, 152.8, 158.7, and 167.8; anal. calcd for $C_{22}H_{20}IN_3O_5$ (m.w. 533.32): C, 49.55; H, 3.78; and N, 7.88. Found: C, 49.47; H, 3.86; and N, 7.79.

4.1.3. 2-[1-Allyl-6-iodo-2,4-dioxo-1,4-dihydroquinazolin-3(2*H*)-yl]-*N*-[4-(hydrazinecarbonyl)phenyl]acetamide (7).

Hydrazine hydrate 100% (0.5 mL, 0.01 mol) was added dropwise to a stirred solution of compound **6b** (0.002 mol) in absolute ethanol (20 mL). The mixture was stirred well and heated under reflux for 6 h. The reaction mixture was cooled, and the crude product was filtered and recrystallized from ethanol.

Yield, 80%; m.p. 297–9 °C; $IR_{\nu max}$ (cm^{-1}): 3250, 3200, 3117 (2NH & NH$_2$), 1710, and 1685 (4C=O); ^{13}C-NMR (100 MHz, DMSO-d_6): 52.5, 53.8, 95.7, 104.4, 122.6 (2), 124.1, 127.6, 128.1, 129.8 (3), 136.7, 138.6, 139.4, 149.0, 152.6, 158.6, 160.3, and 160.7; anal. calcd for $C_{20}H_{18}IN_5O_4$ (m.w. 519.30): C, 46.26; H, 3.49; and N, 13.49. Found: C, 46.30; H, 3.55; and N, 13.54.

4.1.4. 2-(1-Allyl-6-iodo-2,4-dioxo-1,4-dihydroquinazolin-3(2*H*)-yl)-*N*-(4-(5-mercapto-1,3,4-oxadiazol-2-yl)phenyl) acetamide (8).

Compound 7 (5.19 g, 0.01 mol) was dissolved in a solution of potassium hydroxide (0.56 g, 0.01 mol) in ethanol (40 mL) and water (2 mL). Carbon disulphide (3 mL, 4.61 g, 0.06 mol) was then added while stirring, and the reaction mixture was refluxed for 24 h. The reaction mixture was concentrated, cooled to room temperature and acidified with dil. HCl. The obtained precipitate was filtered, washed with water and crystallized from ethanol to give the title compound **8**.

Yield, 76%; m.p. 288–9 °C; $IR_{\nu max}$ (cm^{-1}): 3234, 3179 (2NH), 1685, 1670 (3C=O), and 1255 (C=S); ^{1}H-NMR (400 MHz, DMSO-d_6): 4.69 (s, 2H, C**H**$_2$CO), 5.08–5.17 (m, 2CH$_2$, C**H**$_2$CH & C**H**$_2$=CH), 5.84–5.97 (m, 1H, C**H**=CH$_2$), 7.23–8.02 (m, 7H, 7Ar–H), 11.57 (s, 1H, NH, D_2O exchangeable), and 13.79 (s, 1H, SH, D_2O exchangeable); ^{13}C-NMR (100 MHz, DMSO-d_6): 51.5, 53.2, 94.4, 112.4, 116.6, 120.0 (2), 125.6, 130.7 (3), 131.4, 133.2, 134.6, 142.9, 148.7, 154.9, 158.9, 165.4, 167.3, and 167.7; anal. calcd for $C_{21}H_{16}IN_5O_4S$ (561.35): C, 44.93; H, 2.87; and N, 12.48. Found: C, 45.05; H, 2.80; and N, 12.54.

4.1.5. 2-[1-Allyl-6-iodo-2,4-dioxo-1,4-dihydroquinazolin-3(2*H*)-yl]-*N*-[4-(5-methyl-1,3,4-oxadiazol-2-yl)phenyl]acetamide (9).

Compound 7 (1.00 g, 0.002 mol) was refluxed with acetic

anhydride (10 mL) for 3 h, then the reaction mixture was allowed to attain room temperature. The reaction mixture was poured on crushed ice, and the formed precipitate was filtered and crystallized from ethanol to give the target compound **9**.

Yield, 78%; m.p. 295–7 °C; IR_{vmax} (cm^{-1}): 3315 (NH), 1703, and 1659 (3C=O); ^{1}H-NMR (400 MHz, DMSO-d_6): 2.72 (s, 3H, CH_3), 4.75–4.77 (s, $2CH_2$, C**H**$_2$CO & C**H**$_2$CH), 5.13–5.14 (m, 2H, C**H**$_2$ = CH), 5.87–5.90 (m, 1H, C**H**=CH_2), 7.58–8.04 (m, 7H, 7Ar–H), and 10.50 (s, 1H, NH, D_2O exchangeable); ^{13}C-NMR (100 MHz, DMSO-d_6): 22.7, 53.5, 55.2, 95.3, 110.3, 114.2, 117.9, 124.1 (2), 125.3, 130.5 (3), 130.9, 132.2, 133.5, 142.5, 147.5, 153.8, 159.8, 167.8, and 168.4; anal. calcd for $C_{22}H_{18}IN_5O_4$ (543.32): C, 48.63; H, 3.34; and N, 12.89. Found: C, 48.58; H, 3.30; and N, 12.96.

4.1.6. 2-[1-Allyl-6-iodo-2,4-dioxo-1,4-dihydroquinazolin-3(2*H*)-yl]-*N*-[4-(3,5-dimethyl-1*H*-pyrazol-1-yl)phenyl]acetamide (10). Acetylacetone (0.20 mL, 0.20 g, 0.002 mol) was added to a solution of compound **8** (1.00 g, 0.002 mol) in dioxane (20 mL) and few drops of TEA. The reaction mixture was refluxed for 4 h, concentrated, and cooled to room temperature, and the precipitate was filtered and crystallized from ethanol to give compound **10**.

Yield, 72%; m.p. 297–9 °C; IR_{vmax} (cm^{-1}): 3316 (NH), 1734, 1701, and 1660 (3C=O); ^{1}H-NMR (400 MHz, DMSO-d_6): 1.99 (s, 3H, CH_3 at position-5 of pyrazole), 2.19 (s, 3H, CH_3 at position-3 of pyrazole), 4.79–4.83 (s, $2CH_2$, C**H**$_2$CO & C**H**$_2$CH), 5.12–5.21 (m, 2H, C**H**$_2$=CH), 5.84–5.98 (m, 1H, C**H**=CH_2), 6.22 (s, 1H, CH pyrazole), 7.31–8.10 (m, 7H, 7Ar–H), and 10.67 (s, 1H, NH, D_2O exchangeable); ^{13}C-NMR (100 MHz, DMSO-d_6): 12.7, 15.8, 50.8, 54.7, 97.3, 111.9, 118.3, 118.8, 120.3 (2), 126.9, 127.5, 129.6 (3), 134.1, 139.0, 142.6, 152.6, 157.9, 162.3, 156.3, 168.0, and 171.9; anal. calcd for $C_{24}H_{22}IN_5O_3$ (555.38): C, 51.90; H, 3.99; and N, 12.61. Found: C, 52.02; H, 4.04; and N, 12.58.

4.1.7. 4-{2-[1-Benzyl-6-iodo-2,4-dioxo-1,4-dihydroquinazolin-3(2*H*)-yl]acetamido}-*N*-methylbenzamide (13)

4.1.7.1. General method. A mixture of equimolar quantities of 1-benzyl-6-iodoquinazoline-2,4(1*H*,3*H*)-dione (**12**) (3.78 g, 0.01 mol) and 4-(2-chloroacetamido)-*N*-methyllbenzamide (**IIIa**) (2.26 g, 0.01 mol) in dry acetone (50 mL) was heated under reflux for 12 h in the presence of K_2CO_3 (1.38 g, 0.01 mol). The reaction mixture was filtered off while hot. The precipitated solids were filtered, dried and crystallized from ethanol to give the corresponding target compound **13**.

Yield, 75%; m.p. 292–4 °C; IR_{vmax} (cm^{-1}): 3283, 3230 (2NH), 1692, 1658, and 1653 (4C=O); ^{1}H-NMR (400 MHz, DMSO-d_6): 3.06 (s, 3H, NHC**H**$_3$), 4.88 (s, 2H, C**H**$_2$CO), 5.43 (s, 2H, NC**H**$_2$), 7.03–8.12 (m, 12H, 12Ar–H), 9.75 (s, 1H, **NH**CH_3 (D_2O exchangeable)), and 10.61 (s, 1H, NH, D_2O exchangeable); ^{13}C-NMR (100 MHz, DMSO-d_6): 24.7, 52.1, 55.9, 118.9, 120.0 (2), 121.4, 124.9 (3), 129.5 (2), 129.9, 130.5, 130.7, 131.3 (2), 133.3, 134.2 (2), 142.0, 144.2, 164.8, 165.8, and 167.6; anal. calcd for $C_{25}H_{21}IN_4O_4$ (m.w. 568.37): C, 52.83; H, 3.72; and N, 9.86. Found: C, 52.77; H, 3.68; and N, 9.90.

4.1.8. Alkyl 4-{2-[1-benzyl-6-iodo-2,4-dioxo-1,4-dihydroquinazolin-3(2*H*)-yl]acetamido}benzoate (14a,b)

4.1.8.1. General method. A mixture of equimolar quantities of 1-benzyl-6-iodoquinazoline-2,4(1*H*,3*H*)-dione (**12**) (3.78 g, 0.01 mol) and appropriate alkyl 4-(2-chloroacetamido)benzoate **IIb,c** (0.01 mol) in dry acetone (50 mL) was heated under reflux for 12 h in the presence of K_2CO_3 (1.38 g, 0.01 mol). The reaction mixture was filtered off while hot. The precipitated solids were filtered, dried and crystallized from ethanol to give corresponding target compounds **14a,b**.

*4.1.8.2. Methyl 4-{2-[1-benzyl-6-iodo-2,4-dioxo-1,4-dihydroquinazolin-3(2H)-yl]acetamido}benzoate (**14a**).* Yield, 70%; m.p. 272–4 °C; IR_{vmax} (cm^{-1}): 3385 (NH), 1751, 1734, 1697, and 1685 (4C=O); ^{1}H-NMR (400 MHz, DMSO-d_6): 3.79 (s, 3H, COOC**H**$_3$), 4.84 (s, 2H, C**H**$_2$CO), 5.39 (s, 2H, NC**H**$_2$), 7.29–7.89 (m, 12H, 12Ar–H), and 10.68 (s, 1H, NH, D_2O exchangeable); ^{13}C-NMR (100 MHz, DMSO-d_6): 33.0, 54.7, 57.1, 96.3, 109.4, 112.7, 117.1, 122.6 (2), 124.1 (3), 126.3, 129.7 (2), 132.3 (2), 137.1 (2), 141.2, 149.6, 153.1, 158.7, 166.1, and 170.7; anal. calcd for $C_{25}H_{20}IN_3O_5$ (m.w. 569.36): C, 52.74; H, 3.54; and N, 7.38. Found: C, 52.70; H, 3.51; and N, 7.44.

*4.1.8.3. Ethyl 4-{2-[1-benzyl-6-iodo-2,4-dioxo-1,4-dihydroquinazolin-3(2H)-yl]acetamido}benzoate (**14b**).* Yield, 75%; m.p. 277–9 °C; IR_{vmax} (cm^{-1}): 3262 (NH), 1722, 1697, 1666, and 1652 (4C=O); ^{1}H-NMR (400 MHz, DMSO-d_6): 1.26–1.29 (t, 3H, CH_2C**H**$_3$), 4.24–4.27 (q, 2H, C**H**$_2$$CH_3$), 4.84 (s, 2H, C**H**$_2$CO), 5.38 (s, 2H, NC**H**$_2$), 7.23–7.91 (m, 12H, 12Ar–H), and 10.67 (s, 1H, NH, D_2O exchangeable); anal. calcd for $C_{26}H_{22}IN_3O_5$ (m.w. 583.38): C, 53.53; H, 3.80; and N, 7.20. Found: C, 53.50; H, 3.70; and N, 7.28.

4.1.9. 2-[1-Benzyl-6-iodo-2,4-dioxo-1,4-dihydroquinazolin-3(2*H*)-yl]-*N*-[4-(hydrazinecarbonyl)phenyl]acetamide (15). Hydrazine hydrate 100% (0.5 mL, 0.01 mol) was added dropwise to a stirred solution of compound **14b** (1.17 g, 0.002 mol) in absolute ethanol (20 mL). The mixture was stirred well and heated at 70 °C for 6 h. The reaction mixture was cooled, and the crude product was filtered and recrystallized from ethanol.

Yield, 84%; m.p. 300–2 °C; IR_{vmax} (cm^{-1}): 3290, 3262, 3184 (2NH & NH_2), 1733, and 1665 (4C=O); ^{1}H-NMR (400 MHz, DMSO-d_6): 4.89 (s, 2H, C**H**$_2$CO), 5.43 (s, 2H, NC**H**$_2$), 6.65 (s, 2H, N**H**$_2$), 7.26–8.12 (m, 12H, 12Ar–H), 10.63 (s, 1H, N**H**NH_2, D_2O exchangeable), and 12.03 (s, 1H, CONH, D_2O exchangeable); anal. calcd for $C_{24}H_{20}IN_5O_4$ (m.w. 569.36): C, 50.63; H, 3.54; and N, 12.30. Found: C, 50.55; H, 3.60; and N, 12.42.

4.1.10. 2-[1-Benzyl-6-iodo-2,4-dioxo-1,4-dihydroquinazolin-3(2*H*)-yl]-*N*-[4-(5-mercapto-1,3,4-oxadiazol-2-yl)phenyl] acetamide (16). Compound **15** (5.69 g, 0.01 mol) was dissolved in a solution of potassium hydroxide (0.56 g, 0.01 mol) in ethanol (40 mL) and water (2 mL). Carbon disulphide (3 mL, 4.61 g, 0.06 mol) was then added while stirring, and the reaction mixture was refluxed for 24 h. The reaction mixture was concentrated, cooled to room temperature and acidified with dil. HCl. The obtained precipitate was filtered, washed with water and crystallized from ethanol to give the title compound **16**.

Yield, 78%; m.p. 297–9 °C; IR_{vmax} (cm^{-1}): 3313, 3255 (2NH), 1700, 1675, 1636 (3C=O), and 1260 (C=S); ^{1}H-NMR (400 MHz, DMSO-d_6): 4.89 (s, 2H, C**H**$_2$CO), 5.42 (s, 2H, NC**H**$_2$), 7.26–8.09 (m, 12H, 12Ar–H), 10.70 (s, 1H, NH, D_2O exchangeable), and 14.60 (s, 1H, SH, D_2O exchangeable); anal. calcd for $C_{25}H_{18}IN_5O_4S$ (611.41): C, 49.11; H, 2.97; and N, 11.45. Found: C, 49.00; H, 3.04; and N, 11.38.

4.1.11. 2-[1-Benzyl-6-iodo-2,4-dioxo-1,4-dihydroquinazolin-3(2*H*)-yl]-*N*-[4-(5-methyl-1,3,4-oxadiazol-2-yl)phenyl]acetamide (17). Compound **15** (1.00 g, 0.002 mol) was refluxed with acetic anhydride (10 mL) for 3 h, then the reaction mixture was allowed to attain room temperature. The reaction mixture was poured on crushed ice, and the formed precipitate was filtered and crystallized from ethanol to give the target compound **17**.

Yield, 74%; m.p. 305–7 °C; IR_{vmax} (cm^{-1}): 3318 (NH), 1733, 1686, and 1671 (3C=O); ^{1}H-NMR (400 MHz, DMSO-d_6): 3.30 (s, 3H, CH_3), 4.85 (s, 2H, C**H**$_2$CO), 5.39 (s, 2H, NC**H**$_2$), 7.33–8.11 (m, 12H, 12Ar–H), and 10.63 (s, 1H, NH, D_2O exchangeable); ^{13}C-NMR (100 MHz, DMSO-d_6): 20.1, 52.4, 54.7, 93.4, 112.0, 116.8 (2), 121.4 (3), 124.3 (2), 126.9, 129.7 (2), 134.5 (2), 139.0, 144.1, 148.2, 152.0, 154.7, 158.4, 162.9, 167.2, and 171.8; anal. calcd for $C_{26}H_{20}IN_5O_4$ (593.38): C, 52.63; H, 3.40; and N, 11.80. Found: C, 52.58; H, 3.36; and N, 11.74.

4.1.12. 2-[1-Benzyl-6-iodo-2,4-dioxo-1,4-dihydroquinazolin-3(2*H*)-yl]-*N*-[4-(3,5-dimethyl-1*H*-pyrazol-1-yl)phenyl]acetamide (18). Acetylacetone (0.20 mL, 0.20 g, 0.002 mol) was added to a solution of compound **15** (1.00 g, 0.002 mol) in dioxane (20 mL) and few drops of TEA. The reaction mixture was refluxed for 4 h, concentrated, and cooled to room temperature, and the precipitate was filtered and crystallized from ethanol to give compound **18**.

Yield, 70%; m.p. 310–2 °C; IR_{vmax} (cm^{-1}): 3310 (NH), 1722, 1697, and 1666 (3C=O); ^{1}H-NMR (400 MHz, DMSO-d_6): 2.17 (s, 3H, CH_3 at position-5 of pyrazole), 2.53 (s, 3H, CH_3 at position-3 of pyrazole), 4.89 (s, 2H, C**H**$_2$CO), 5.42 (s, 2H, NC**H**$_2$), 6.26 (s, 1H, CH pyrazole), 7.29–7.94 (m, 12H, 12Ar–H), and 10.69 (s, 1H, NH, D_2O exchangeable); ^{13}C-NMR (100 MHz, DMSO-d_6): 14.4, 18.3, 51.5, 55.8, 95.8, 108.8, 112.3 (2), 115.8 (3), 119.7 (2), 122.7 (2), 126.7, 128.1, 129.8 (2), 130.5, 139.5, 141.9, 146.7, 149.1, 153.0, 162.1, 166.3, and 172.5; anal. calcd for $C_{28}H_{24}IN_5O_3$ (605.44): C, 55.55; H, 4.00; and N, 11.57. Found: C, 55.50; H, 3.94; and N, 11.49.

4.2. Docking studies

EGFR^{WT} (PDB: 4HJO)[41] and EGFR^{T790M} (PDB: 3W2O)[38] were used with the Molsoft program to carry out docking studies.

4.3. Biological testing

4.3.1. *In vitro* anticancer activity. Our derivatives **3–14** were tested against four cell lines, HCT116, HepG2, MCF-7 and A549, using MTT colorimetric assay.[42,43]

4.3.2. *In vitro* EGFR^{WT} assay. All compounds were assessed for their inhibitory activities against VEGFR-2.[44]

4.3.3. EGFR^{T790M} assay. Using the HTRF assay, all drugs were assessed for their ability to inhibit mutant EGFR^{T790M}.[44,45]

Author contributions

K. El-Adl, Hanan Osman, Basmah Almohaywi, Samy Mohamady, Ahmed Aljohani, Ahmed El-morsy, and Marwa Alsulaimany were responsible for the conception and rational design of the work. K. El-Adl, Samy Mohamady, Ahmed Aljohani, Omar Alatawi and Marwa Alsulaimany were responsible for the data collection and synthesis of the new compounds. K. El-Adl and Majed Aljohani performed the molecular docking study. K. El-Adl, Hussam Alharbi, Basmah Almohaywi, Ahmed El-morsy, Ahmed Aljohani and Marwa Alsulaimany were responsible for spectral data analysis. Felemban Athary Abdulhaleem, Sara Almadani, Basmah Almohaywi, Hanan Osman and K. El-Adl conducted the cytotoxicity assay. Sara Almadani, Felemban Athary Abdulhaleem, Hanan Osman and K. El-Adl conducted the *in silico* pharmacokinetic study. All authors discussed the results and contributed to the writing and revision of the original manuscript.

Conflicts of interest

The authors declare that they have no known competing financial interests or personal relationships that could have appeared to influence the work reported in this paper.

Acknowledgements

The authors express their gratitude and admiration to Dr Mohamed Morsy, Faculty of Science, Al-Azhar University for supporting the pharmacological part.

References

1 M. T. Ibrahim, A. Uzairu, S. Uba, *et al.*, Design of more potent quinazoline derivatives as EGFRWT inhibitors for the treatment of NSCLC: a computational approach, *Future J. Pharm. Sci.*, 2021, **7**, 140, DOI: **10.1186/s43094-021-00279-3**.

2 S. Turker, H. Sahinli, P. Perkin, D. Yazilitas, N. O. Koklu, G. I. Imamoglu and C. Karacin, Altinbas M "Squamos cell lung cancer" case applying with dyspepsia complaints, *J. Oncol. Sci.*, 2018, **4**(3), 147–148.

3 A. Arora and E. M. Scholar, Role of tyrosine kinase inhibitors in cancer therapy, *J. Pharmacol. Exp. Ther.*, 2005, **315**, 971–979.

4 S. S. Zahran, F. A. Ragab, M. G. El-Gazzar, A. M. Soliman, W. R. Mahmoud and M. M. Ghorab, Antiproliferative, antiangiogenic and apoptotic effect of new hybrids of quinazoline-4 (3H)-ones and sulfachloropyridazine, *Eur. J. Med. Chem.*, 2023, **245**, 114912.

5 B. Zhao, Z. Xiao, J. Qi, R. Luo, Z. Lan, Y. Zhang, X. Hu, Q. Tang, P. Zheng and S. Xu, Design, synthesis and biological evaluation of AZD9291 derivatives as selective and potent EGFRL858R/T790M inhibitors, *Eur. J. Med. Chem.*, 2019, **163**, 367–380, DOI: **10.1016/j.ejmech.2018.11.069**.

6 B. A. Chan, Hughes BG Targeted therapy for non-small cell lung cancer: current standards and the promise of the future, *Transl. Lung Cancer Res.*, 2015, **4**(1), 36.

7 S. Kobayashi, T. J. Boggon, T. Dayaram, P. A. Jänne, O. Kocher, M. Meyerson, B. E. Johnson, M. J. Eck, D. G. Tenen and B. Halmos, EGFR mutation and resistance of non–small-cell lung cancer to gefitinib, *N. Engl. J. Med.*, 2005, **352**(8), 786–792, DOI: **10.1056/NEJMoa044238**.

8 W. Zhou, D. Ercan, L. Chen, C.-H. Yun, D. Li, M. Capelletti, A. B. Cortot, L. Chirieac, R. E. Iacob and R. Padera, Novel mutant-selective EGFR kinase inhibitors against EGFR

T790M, *Nature*, 2009, **462**(7276), 1070–1074, DOI: 10.1038/nature08622.

9 S. A. Elmetwally, K. F. Saied, I. H. Eissa and E. B. Elkaeed, Design, synthesis and anticancer evaluation of thieno[2,3-d]pyrimidine derivatives as dual EGFR/HER2 inhibitors and apoptosis inducers, *Bioorg. Chem.*, 2019, **88**, 102944, DOI: 10.1016/j.bioorg.2019.102944.

10 A. A. Nasser, I. H. Eissa, M. R. Oun, M. A. El-Zahabi, M. S. Taghour, A. Belal, A. M. Saleh, A. B. M. Mehany, H. Luesch, A. E. Mostafa, W. M. Afifi, J. R. Rocca and H. A. Mahdy, Discovery of new pyrimidine-5-carbonitrile derivatives as anticancer agents targeting EGFRWT and EGFRT790M, *Org. Biomol. Chem.*, 2020, **18**(38), 7608–7634, DOI: 10.1039/D0OB01557A.

11 Y. Harada, A. Sato, H. Nakamura, *et al.*, Anti-cancer effect of afatinib, dual inhibitor of HER2 and EGFR, on novel mutation HER2 E401G in models of patient-derived cancer, *BMC Cancer*, 2023, **3**, 77, DOI: 10.1186/s12885-022-10428-3.

12 D. Lavacchi, F. Mazzoni and G. Giaccone, Clinical evaluation of dacomitinib for the treatment of metastatic non-small cell lung cancer (NSCLC): current perspectives, *Drug Des., Dev. Ther.*, 2019, **13**, 3187–3198, DOI: 10.2147/DDDT.S194231.

13 D. A. Cross, S. E. Ashton, S. Ghiorghiu, C. Eberlein, C. A. Nebhan, P. J. Spitzler, J. P. Orme, M. R. Finlay, R. A. Ward, M. J. Mellor, G. Hughes, A. Rahi, V. N. Jacobs, M. Red Brewer, E. Ichihara, J. Sun, H. Jin, P. Ballard, K. Al-Kadhimi, R. Rowlinson, T. Klinowska, G. H. Richmond, M. Cantarini, D. W. Kim, M. R. Ranson and W. Pao, AZD9291, an irreversible EGFR TKI, overcomes T790M-mediated resistance to EGFR inhibitors in lung cancer, *Cancer Discovery*, 2014, **4**(9), 1046–1061, DOI: 10.1158/2159-8290.CD-14-0337.

14 R. Pawara, I. Ahmad, D. Nayak, S. Belamkar, S. Surana, C. N. Kundu, C. Patil and H. Patel, Design and synthesis of the novel, selective WZ4002 analogue as EGFR-L858R/T790M tyrosine kinase inhibitors for targeted drug therapy in non-small-cell lung cancer (NSCLC), *J. Mol. Struct.*, 2022, **1254**, 132313, DOI: 10.1016/j.molstruc.2021.132313.

15 A. G. A. El-Helby, H. Sakr, I. H. Eissa, H. Abulkhair, A. A. Al-Karmalawy and K. El-Adl, Design, synthesis, molecular docking, and anticancer activity of benzoxazole derivatives as VEGFR-2 inhibitors, *Arch. Pharm.*, 2019, **352**, 1900113.

16 M. A. Abdelgawad, K. El-Adl, S. S. El-Hddad, M. M. Elhady, N. M. Saleh, M. M. Khalifa, F. Khedr, M. Alswah, A. A. Nayl and M. M. Ghoneim, Design, molecular docking, synthesis, anticancer and anti-hyperglycemic assessments of thiazolidine-2, 4-diones Bearing Sulfonylthiourea Moieties as Potent VEGFR-2 Inhibitors and PPARγ Agonists, *Pharmaceuticals*, 2022, **15**, 226.

17 F. Khedr, M.-K. Ibrahim, I. H. Eissa, H. S. Abulkhair and K. El-Adl, Phthalazine-based VEGFR-2 inhibitors: Rationale, design, synthesis, in silico, ADMET profile, docking, and anticancer evaluations, *Arch. Pharm.*, 2021, e2100201, DOI: 10.1002/ardp.202100201.

18 A. G. A. El-Helby, R. R. Ayyad, H. Sakr, K. El-Adl, M. M. Ali and F. Khedr, design, synthesis, molecular docking, and anticancer activity of phthalazine derivatives as VEGFR-2 inhibitors, *Arch. Pharm.*, 2017, **350**, 1700240.

19 M. M. Ghorab, A. M. Soliman, K. El-Adl and N. S. Hanafy, New quinazoline sulfonamide derivatives as potential anticancer agents: Identifying a promising hit with dual EGFR/VEGFR-2 inhibitory and radiosensitizing activity, *Bioorg. Chem.*, 2023, **140**, 106791, DOI: 10.1016/j.bioorg.2023.106791.

20 M. A. El-Zahabi, H. Sakr, K. El-Adl, M. Zayed, A. S. Abdelraheem, S. I. Eissa, H. Elkady and I. H. Eissa, Design, synthesis, and biological evaluation of new challenging thalidomide analogs as potential anticancer immunomodulatory agents, *Bioorg. Chem.*, 2020, **104**, 104218, DOI: 10.1016/j.bioorg.2020.104218.

21 N. M. Saleh, M. S. A. El-Gaby, K. El-Adl and N. E. A. Abd El-Sattar, Design, green synthesis, molecular docking and anticancer evaluations of diazepam bearing sulfonamide moieties as VEGFR-2 inhibitors, *Bioorg. Chem.*, 2020, **104**, 104350, DOI: 10.1016/j.bioorg.2020.104350.

22 A. E. Abdallah, I. H. Eissa, A. B. M. Mehany, H. Sakr, A. Atwa, K. El-Adl and M. A. El-Zahabi, Immunomodulatory quinazoline-based thalidomide analogs: Design, synthesis, apoptosis and anticancer evaluations, *J. Mol. Struct.*, 2023, **1281**, 135164, DOI: 10.1016/j.molstruc.2023.135164.

23 N. S. Hanafy, N. A. A. M. Aziz, S. S. A. El-Hddad, M. A. Abdelgawad, M. M. Ghoneim, A. F. Dawood, S. Mohamady, K. El-Adl and S. Ahmed, Design, synthesis, and docking of novel thiazolidine-2,4-dione multitarget scaffold as new approach for cancer treatment, *Arch. Pharm.*, 2023, e2300137, DOI: 10.1002/ardp.202300137.

24 D. Adel, K. El-Adl, T. Nasr, T. M. Sakr and W. Zaghary, Pyrazolo[3,4-d]pyrimidine derivatives as EGFRT790M and VEGFR-2 dual TK inhibitors: Design, synthesis, molecular docking, ADMET profile and anticancer evaluations, *J. Mol. Struct.*, 2023, **1291**, 136047, DOI: 10.1016/j.molstruc.2023.136047.

25 H. Elkady, K. El-Adl, H. Sakr, A. S. Abdelraheem, S. I. Eissa and M. A. El-Zahabi, Novel promising benzoxazole/benzothiazole-derived immunomodulatory agents: Design, synthesis, anticancer evaluation, and in silico ADMET analysis, *Arch. Pharm.*, 2023, e2300097, DOI: 10.1002/ardp.202300097.

26 M. A. El-Zahabi, H. Elkady, H. Sakr, A. S. Abdelraheem, S. I. Eissa and K. El-Adl, Design, synthesis, anticancer evaluation, in silico docking and ADMET analysis of novel indole-based thalidomide analogs as promising immunomodulatory agents, *J. Biomol. Struct. Dyn.*, 2023, 1–18, DOI: 10.1080/07391102.2023.2187217.

27 M. Alsulaimany, K. El-Adl, A. K. B. Aljohani, H. Y. Alharbi, O. M. Alatawi, M. S. Aljohani, A. El-Morsy, S. A. Almadani, A. A. Alsimaree, S. A. Salama, D. E. Keshek and A. A. Mohamed, Design, synthesis, docking, ADMET and anticancer evaluations of *N*-alkyl substituted iodoquinazoline derivatives as dual VEGFR-2 and EGFR inhibitors, *RSC Adv.*, 2023, **13**(51), 36301–36321, DOI: 10.1039/d3ra07700d.

28 K. E. Anwer, S. S. A. El-Hddad, N. E. A. Abd El-Sattar, A. M. El-Morsy, F. Khedr, S. Mohamady, D. E. G. Keshek, S. A. Salama, K. El-Adl and N. SHanafy, Five and six membered heterocyclic rings endowed with azobenzene as dual EGFRT790M and VEGFR-2 inhibitors: design, synthesis, in silico ADMET profile, molecular docking, dynamic simulation and anticancer evaluations, *RSC Adv.*, 2023, **13**, 35321–35338, https://api.semanticscholar.org/CorpusID:265657522.

29 M. S. A. El-Gaby, M. A. M. Abdel Reheim, Z. S. M. Akrim, B. H. Naguib, N. M. Saleh, A. A. A. M. El-Adasy, K. El-Adl and S. Mohamady, 2-Thioxo-3,4-dihydropyrimidine and Thiourea Endowed with Sulfonamide Moieties as Dual EGFRT790M and VEGFR-2 Inhibitors: Design, Synthesis, Docking and Anticancer Evaluations, *Drug Dev. Res.*, 2024, **85**, e22143, DOI: 10.1002/ddr.22143.

30 A. A. Mohamed, S. S. A. El-Hddad, A. K. B. Aljohani, F. Khedr, O. M. Alatawi, D. E. Keshek, S. Ahmed, M. Alsulaimany, S. A. Almadani, K. El-Adl and N. S. Hanafy, Iodoquinazoline-derived VEGFR-2 and EGFRT790M dual inhibitors: Design, synthesis, molecular docking and anticancer evaluations, *Bioorg. Chem.*, 2024, **143**, 107062, DOI: 10.1016/j.bioorg.2023.107062.

31 Y. T. Tseng, Y. H. Tsai, F. Fülöp, F. R. Chang and Y. C. Lo, 2-Iodo-4'-Methoxychalcone Attenuates Methylglyoxal-Induced Neurotoxicity by Activation of GLP-1 Receptor and Enhancement of Neurotrophic Signal, Antioxidant Defense and Glyoxalase Pathway, *Molecules*, 2019, **24**(12), 2249, DOI: 10.3390/molecules24122249.

32 Y. Liu and N. S. Gray, Rational design of inhibitors that bind to inactive kinase conformations, *Nat. Chem. Biol.*, 2006, **2**, 358–364.

33 C.-W. Yu, P.-Y. Hung, H. Yang, Y.-H. Ho, H.-Y. Lai, Y.-S. Cheng and J.-W. Chern, Quinazolin-2,4-dione-Based Hydroxamic Acids as Selective Histone Deacetylase-6 Inhibitors for Treatment of Non-Small Cell Lung Cancer, *J. Med. Chem.*, 2019, **62**(2), 857–874, DOI: 10.1021/acs.jmedchem.8b01590.

34 M. El-Naggar, H. R. M. Rashdan and A. H. Abdelmonsef, Cyclization of Chalcone Derivatives: Design, Synthesis, In Silico Docking Study, and Biological Evaluation of New Quinazolin-2,4-diones Incorporating Five-, Six-, and Seven-Membered Ring Moieties as Potent Antibacterial Inhibitors, *ACS Omega*, 2023, **8**(30), 27216–27230, DOI: 10.1021/acsomega.3c02478.

35 H. Chen, P. Li, R. Qin, H. Yan, G. Li and H. Huang, DMAP-Catalyzed One-Pot Synthesis of Quinazoline-2,4-diones from 2-Aminobenzamides and Di-tert-butyl Dicarbonate, *ACS Omega*, 2020, **5**(16), 9614–9623, DOI: 10.1021/acsomega.0c01104.

36 T. Yamashiro, K. Tokushige and T. Abe, One-Pot Synthesis of Core Structure of Shewanelline C Using an Azidoindoline, *J. Org. Chem.*, 2023, **88**(6), 3992–3997, DOI: 10.1021/acs.joc.3c00013.

37 L. Zhang, Q. Chen, L. Li, N. Ma, J. Tian, H. Sun, Q. Xu, Y. Yang and C. Li, Synthesis of *N*-Unsubstituted and N3-Substituted Quinazoline-2,4(1*H*,3*H*)-diones from o-Aminobenzamides and CO2 at Atmospheric Pressure and Room Temperature, *Org. Lett.*, 2023, **25**(14), 2471–2475, DOI: 10.1021/acs.orglett.3c00614.

38 N. A. A. M. Aziz, R. F. George, K. El-Adl and W. R. Mahmoud, Design, synthesis, in silico docking, ADMET and anticancer evaluations of thiazolidine-2,4-diones bearing heterocyclic rings as dual VEGFR-2/EGFRT790M tyrosine kinase inhibitors, *RSC Adv.*, 2022, **12**(20), 12913–12931, DOI: 10.1039/D2RA01119K.

39 N. A. A. M. Aziz, R. F. George, K. El-Adl and W. R. Mahmoud, Exploration of thiazolidine-2,4-diones as tyrosine kinase inhibitors: Design, synthesis, ADMET, docking, and antiproliferative evaluations, *Arch. Pharm.*, 2023, **356**(3), e2200465, DOI: 10.1002/ardp.202200465.

40 K. El-Adl, A.-G. A. El-Helby, H. Sakr and S. S. A. El-Hddad, Design, synthesis, molecular docking, and anticancer evaluations of 1-benzylquinazoline-2,4(1H,3H)-dione bearing different moieties as VEGFR-2 inhibitors, *Arch. Pharm.*, 2020, **353**(8), e2000068, DOI: 10.1002/ardp.202000068.

41 J. H. Park, Y. Liu, M. A. Lemmon and R. Radhakrishnan, Erlotinib binds both inactive and active conformations of the EGFR tyrosine kinase domain, *Biochem. J.*, 2012, **448**(3), 417–423.

42 T. Mosmann, Rapid colorimetric assay for cellular growth and survival: application to proliferation and cytotoxicity assays, *J. Immunol. Methods*, 1983, **65**(1–2), 55–63.

43 N. E. A. Abd El-Sattar, K. El-Adl, M. A. El-Hashash, S. A. Salama and M. M. Elhady, Design, synthesis, molecular docking and in silico ADMET profile of pyrano [2,3-d]pyrimidine derivatives as antimicrobial and anticancer agents, *Bioorg. Chem.*, 2021, **115**, 105186, DOI: 10.1016/j.bioorg.2021.105186.

44 Y. Jia, C. M. Quinn, A. I. Gagnon and R. Talanian, Homogeneous time-resolved fluorescence and its applications for kinase assays in drug discovery, *Anal. Biochem.*, 2006, **356**(2), 273–281.

45 S. Sogabe, Y. Kawakita, S. Igaki, H. Iwata, H. Miki, D. R. Cary, T. Takagi, S. Takagi, Y. Ohta and T. Ishikawa, Structure-based approach for the discovery of pyrrolo[3, 2-d] pyrimidine-based EGFR T790M/L858R mutant inhibitors, *ACS Med. Chem. Lett.*, 2013, **4**, 201–205.

46 D. E. V. Pires, T. L. Blundell and D. B. Ascher, pkCSM: Predicting Small-Molecule Pharmacokinetic and Toxicity Properties Using Graph-Based Signatures, *J. Med. Chem.*, 2015, **58**, 4066, DOI: 10.1021/acs.jmedchem.5b00104.

47 C. A. Lipinski, F. Lombardo, B. W. Dominy and P. J. Feeney, Experimental and computational approaches to estimate solubility and permeability in drug discovery and development settings, *Adv. Drug Delivery Rev.*, 2012, **64**, 4–17.

48 A. Beig, R. Agbaria and A. Dahan, Oral delivery of lipophilic drugs: the tradeoff between solubility increase and permeability decrease when using cyclodextrin-based formulations, *PLoS One*, 2013, **8**, e68237.